White Rose Research Online

eprints@whiterose.ac.uk
https://eprints.whiterose.ac.uk
Universities of Leeds, Sheffield and York

Deposited via The University of Sheffield.

White Rose Research Online URL for this paper:
https://eprints.whiterose.ac.uk/id/eprint/217765/

Version: Published Version

Article:
Xavier, J.M., Magno, R., Russell, R. et al. (2024) Identification of candidate causal variants and target genes at 41 breast cancer risk loci through differential allelic expression analysis. Scientific Reports, 14. 22526.

https://doi.org/10.1038/s41598-024-72163-y

Reuse
This article is distributed under the terms of the Creative Commons Attribution-NonCommercial-NoDerivs (CC BY-NC-ND) licence. This licence only allows you to download this work and share it with others as long as you credit the authors, but you can't change the article in any way or use it commercially. More information and the full terms of the licence here: https://creativecommons.org/licenses/

Takedown
If you consider content in White Rose Research Online to be in breach of UK law, please notify us by emailing eprints@whiterose.ac.uk including the URL of the record and the reason for the withdrawal request.

UNIVERSITY OF LEEDS
University of Sheffield
UNIVERSITY of York

scientific reports

Check for updates

OPEN

Identification of candidate causal variants and target genes at 41 breast cancer risk loci through differential allelic expression analysis

Joana M. Xavier[1,2]✉, Ramiro Magno[1,8], Roslin Russell[3,9], Bernardo P. de Almeida[4,5,10], Ana Jacinta-Fernandes[4], André Besouro-Duarte[1], Mark Dunning[3,11], Shamith Samarajiwa[6,12], Martin O'Reilly[3], António M. Maia[1], Cátia L. Rocha[4,13], Nordiana Rosli[4,7,14], Bruce A. J. Ponder[3] & Ana-Teresa Maia[1,2,4]✉

Understanding breast cancer genetic risk relies on identifying causal variants and candidate target genes in risk loci identified by genome-wide association studies (GWAS), which remains challenging. Since most loci fall in active gene regulatory regions, we developed a novel approach facilitated by pinpointing the variants with greater regulatory potential in the disease's tissue of origin. Through genome-wide differential allelic expression (DAE) analysis, using microarray data from 64 normal breast tissue samples, we mapped the variants associated with DAE (daeQTLs). Then, we intersected these with GWAS data to reveal candidate risk regulatory variants and analysed their cis-acting regulatory potential. Finally, we validated our approach by extensive functional analysis of the 5q14.1 breast cancer risk locus. We observed widespread gene expression regulation by cis-acting variants in breast tissue, with 65% of coding and noncoding expressed genes displaying DAE (daeGenes). We identified over 54 K daeQTLs for 6761 (26%) daeGenes, including 385 daeGenes harbouring variants previously associated with BC risk. We found 1431 daeQTLs mapped to 93 different loci in strong linkage disequilibrium with risk-associated variants (risk-daeQTLs), suggesting a link between risk-causing variants and cis-regulation. There were 122 risk-daeQTL with stronger cis-acting potential in active regulatory regions with protein binding evidence. These variants mapped to 41 risk loci, of which 29 had no previous report of target genes and were candidates for regulating the expression levels of 65 genes. As validation, we identified and functionally characterised five candidate causal variants at the 5q14.1 risk locus targeting the *ATG10* and *ATP6AP1L* genes, likely acting via modulation of alternative transcription and transcription factor binding. Our study demonstrates the power of DAE analysis and daeQTL mapping to identify causal regulatory variants and target genes at breast cancer risk loci, including those with complex regulatory landscapes. It additionally provides a genome-wide resource of variants associated with DAE for future functional studies.

[1]Cintesis@Rise, Universidade do Algarve, Faro, Portugal. [2]Centro de Ciências do Mar (CCMAR), Universidade do Algarve, Faro, Portugal. [3]Cambridge Institute – CRUK, University of Cambridge, Cambridge, UK. [4]Faculdade de Medicina e Ciências Biomédicas (FMCB), Universidade do Algarve, Faro, Portugal. [5]Faculdade de Medicina, Instituto de Medicina Molecular, Universidade de Lisboa, Lisbon, Portugal. [6]Medical Research Council (MRC) Cancer Unit, Hutchison/MRC Research Centre, University of Cambridge, Cambridge, UK. [7]Training Division, Ministry of Health Malaysia, Putrajaya, Malaysia. [8]Present address: Pattern Institute PT, Faro, Portugal. [9]Present address: Department of Genetics, University of Cambridge, Cambridge, UK. [10]Present address: InstaDeep, Paris, France. [11]Present address: Sheffield Bioinformatics Core, The School of Medicine and Population Health, The University of Sheffield, Sheffield, UK. [12]Present address: Genetics and Genomics Section, Imperial College London, London, UK. [13]Present address: Faculty of Medicine, Instituto de Saúde Ambiental (ISAMB), University of Lisbon, Lisbon, Portugal. [14]Present address: Biometrology Group, Division of Chemical and Biological Metrology, Korea Research Institute of Standards and Science, Daejeon, South Korea. ✉email: jgxavier@ualg.pt; atmaia@ualg.pt

Keywords Cis-regulation, Polymorphism, Cancer predisposition, Breast cancer

Genome-wide association studies (GWAS) for breast cancer (BC) have identified hundreds of risk-associated loci and have generated long lists of candidate loci requiring further validation[1]. Nevertheless, the identification of the causal variants and their target genes, as well as understanding the underlying biological mechanisms, remain challenging. This is because disease risk loci often have many variants in high linkage disequilibrium (LD) with the risk-associated variant, harbour multiple genes and mainly fall in noncoding genome regions[2]. However, the overrepresentation of potential causal variants at active gene regulatory regions[3,4] indicates that variants regulating gene expression levels likely influence BC genetic predisposition, both proximally and over a long range[5–11]. These variants have commonly been mapped by expression quantitative trait loci (eQTL) analysis, but this approach is impacted by the effects of negative feedback control and environmental factors[12]. An increasingly popular alternative approach is to detect imbalances in allelic transcript levels—differential allelic expression (DAE). By comparing the relative expression of the two alleles in a heterozygous individual, each allele will serve as an internal standard for the other, thus controlling for trans-regulatory and environmental factors affecting both alleles[13,14]. Consequently, this directly indicates regulatory variants acting in *cis* (rSNPs).

Given the importance of cis-regulatory variants for BC susceptibility, a genome-wide map of cis-regulatory variants would be key to interpreting GWAS results and identifying causal variants of risk. Studies in various healthy tissues showed that DAE is a relatively common event[13,15–19]. Given that gene expression regulation is tissue-specific, performing these studies in the tissue from which the disease arises, namely, normal breast tissue, is essential. Although others have used allelic expression analysis to identify BC risk, this was carried out in tumour tissue or lymphoblastoid cells[20,21]. This study proposes an integrative approach to identify causal variants of risk that have a cis-regulatory role (Fig. 1): to combine GWAS results with SNPs associated with DAE levels in normal breast tissue. Hence, we first carried out DAE analysis in normal breast tissue samples at a genome-wide level, then mapped the candidate risk regulatory variants for GWAS loci and finally functionally unveiled the mechanisms underlying BC risk at a selected locus.

Methods

SNP and call filtering at the gDNA and cDNA levels

We used an Illumina Infinium Exon510S-Duo arrays dataset of normal breast tissue available from Gene Expression Omnibus (GEO, www.ncbi.nlm.nih.gov/geo/) under accession number GSE35023[22]. It consists of 66 samples of DNA and cDNA (derived from total RNA) run on Illumina Infinium Exon510S-Duo arrays. These exon-centric microarrays contain probes for 511,354 SNPs, with more than 60% of the markers located within 10 kb of a gene and targeting more than 99.9% of human RefSeq genes. Sample filtering and normalisation were performed as described previously, and 12 samples displaying poor dynamic range of intensities in either channel (IQR of non-normalized $\log_2$ X or $\log_2$ Y < 1), or showing evidence of clear contamination of RNA with DNA sample were removed from further analysis[22]. For the remaining 64 samples, we used within-array strip-level quantile normalization to correct for dye-biases between the two channels (in general X = Cy5 = allele A and Y = Cy3 = allele B) from each array to obtain normalized intensities (X* and Y*) for each SNP. The function stripNormalize in the crlmm R package (version 1.10.0) was used to normalize the data. Log-ratios ($M = \log_2 X^* - \log_2 Y^*$) and average log-intensities [$S = 0.5(\log_2 X^* + \log_2 Y^*)$] were then calculated for each SNP on each array. We work on the log-ratio scale rather than the β-scale [$\beta = X^*/(X^* + Y^*)$, as used in Ref.[13], as it has been shown to have more desirable properties for statistical testing in other applications of Infinium technology[23].

Genome-wide DAE analysis

Allelic expression was measured in the filtered dataset of SNPs and samples in a varying number of heterozygous (AB) individuals for each transcribed SNP (aeSNP). As cDNA was prepared from total RNA, without selection for poly-A mRNAs, AE was measured for variants in fully processed and unspliced primary transcripts. Allelic expression ratios (AE ratios) were defined as the $\log_2$ of the ratio between the levels of allele A transcript and the levels of allele B transcript (heterozygote ratio), normalised by the same heterozygote ratio calculated for genomic DNA (gDNA) (Fig. S1), to account for copy number variation and correct for technical biases. Differential allelic expression (DAE) was called at the sample level when AE ratios were greater than 0.58 or less than − 0.58 (corresponding to the $\log_2$ of a 1.5-fold difference between alleles).

To define aeSNPs displaying mono-allelic expression (maeSNPs)[24] we first identified SNPs presenting extreme allelic expression (AE) ratios, specifically with values greater than 0.58 or lower than − 0.58, without any heterozygous samples showing intermediate values. Next, using a binomial test, we tested the distribution of AE ratios at this subset of aeSNPs, displaying extreme ratios for an equal distribution of heterozygous samples showing positive and negative AE ratios on a variant-by-variant basis. We applied multiple testing correction to p-values, and variants with a false discovery rate (FDR) above 5% were considered to display a random choice of expression between alleles and classified as maeSNPs. Genes with at least one maeSNP were labelled maeGenes.

After filtering out maeSNPs, the remaining aeSNPs were tested for differential allelic expression by applying an Equal or Given Proportions test (prop.test function in R), with the alternative hypothesis that the proportion of heterozygotes with absolute AE ratios ≥ 0.58 is greater than 10% for any given SNP. The resulting p-values were corrected using a false discovery rate of 5% to define daeSNPs (Fig. 1, Suppl Fig. S1) i.e., heterozygous transcribed variants displaying differential allelic expression. Genes with at least one daeSNP were henceforth denominated daeGenes.

Validation of nine daeSNPs was performed by TaqMan® PCR technology, as described previously[25], in 25 independent normal breast tissue samples heterozygous for a variable number of individuals per SNP using the following TaqMan® Genotyping Assays predesigned by Applied Biosystems: C___8354687_10; C__29939330_20;

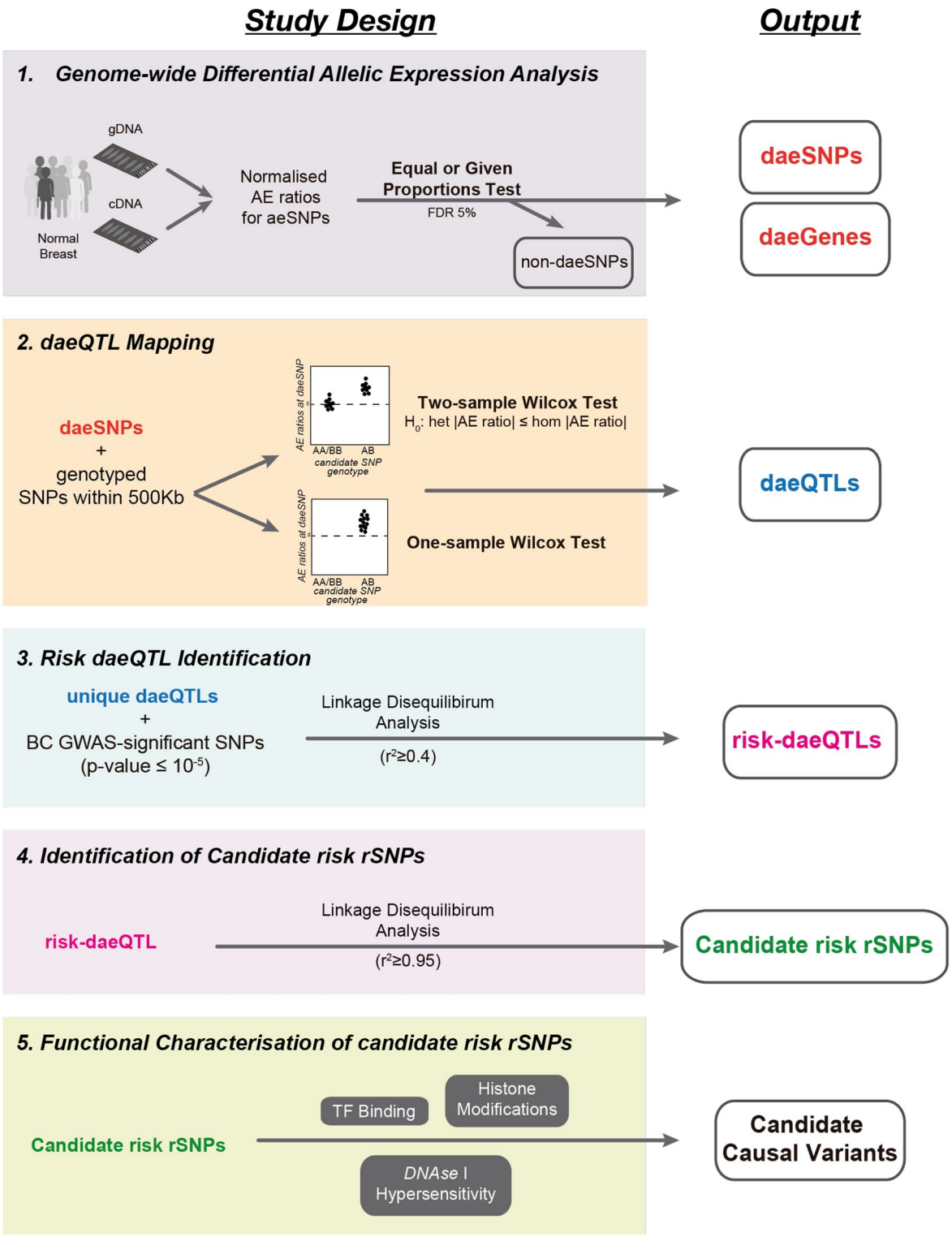

Fig. 1. Strategy framework used to identify causal variants and target genes associated with breast cancer risk. *aeSNP* an SNP that passed quality control and at which allelic expression (AE) was measured, *daeSNP* an aeSNP showing differential AE (DAE), *Genotyped SNP* an SNP with genotype information (either genotyped in the study or imputed) and tested for association with AE ratios, *daeQTL* an SNP associated with AE ratios measured for a daeSNP, *risk-daeQTL* a daeQTL with a $r^2 \geq 0.4$ with a GWAS hit variant, *candidate risk rSNP* a variant with a $r^2 \geq 0.95$ with the risk-daeQTL.

C__31232634_10; C___3133316_10; C__11844169_10; C___2627792_10; C___1517694_1_; C____787630_20; C___3108259_10. The prop.test was equally applied to confirm the presence of differential allelic expression.

Genotype imputation

Imputation was run on the Illumina Exon 510 Duo germline genotype data from the 64 samples that passed microarray quality control filters. Before imputation data, quality control was applied to the genotyping data, and SNPs with call rates < 85%, minor allele frequency < 0.01, and Hardy–Weinberg equilibrium with p-value < 1.0E−05 were excluded from the analysis. Imputation was performed using MACH1.0[26] and the phased haplotypes for HapMap3 release (HapMap3 NCBI Build 36, CEU panel—Utah residents with Northern and Western European ancestry) as a reference panel. We applied the recommended two-step imputation process: model parameters (crossover and error rates) were estimated before imputation using all haplotypes from the study subjects and running 100 iterations of the Hidden Markov Model (HMM) with the command option—greedy and -r 100. Genotype imputation was then carried out using the model parameter estimates from the previous round with command options of -greedy, -mle, and -mldetails specified. Imputation results were assessed by the platform-specific measures of imputation uncertainty for each SNP (rq Score) and filtered for an rq-score ≥ 0.3, as suggested in the author webpage (http://csg.sph.umich.edu/abecasis/mach/tour/) and MAF ≥ 0.01.

This imputation was conducted using HapMap3, which was the most widely used and trusted reference dataset for populations of European ancestry at that time. Since then, more comprehensive reference panels such as the 1000 Genomes Project and the Haplotype Reference Consortium (HRC) have become available, providing improved accuracy. Consequently, for subsequent analyses, including proxy retrieval, we utilized these updated reference panels to enhance the robustness of our findings.

Ancestry analysis

Genetic similarity, as a proxy for global ancestry, was determined by Principal Component Analysis on imputed genotypes from 64 samples, as implemented in PLINK (v.2.00a6LM) using 1000 Genomes Project data (release 20181203) as reference. Data wrangling was performed using bcftools (v.1.10.2, htslib v1.10.2–3).

daeQTL mapping

daeSNPs are not necessarily the regulatory variants (rSNPs) responsible for the observed allelic imbalance. Therefore, mapping of candidate rSNPs associated with the DAE observed—henceforth designated as daeQTLs (differential allelic expression quantitative trait loci) (Fig. S1, Fig. 1) was performed to identify neighboring variants that are statistically associated with the AE ratios observed at the daeSNPs. This approach took into consideration the pattern of AE ratio distribution displayed by each daeSNP. This pattern is highly dependent on the LD between the daeSNP and the rSNP acting upon the gene[27].

To test the association between candidate SNP zygosity and the allelic expression of a daeSNP, henceforth designated daeQTL analysis (differential allelic expression quantitative trait loci analysis), we considered the pattern of the allelic expression (AE) ratio distribution displayed at each daeSNP, as this is dependent on the linkage disequilibrium between the daeSNP and the rSNP. When a single rSNP is in strong LD ($r^2 \sim 1$) with the daeSNP, the normalised AE ratios for all heterozygotes will be unidirectional, with all samples preferentially expressing the same allele (i.e., all samples exhibiting either positive AE ratios or negative AE ratios). In this case, a one-sample Wilcox test was used to compare the mean normalised AE ratios for samples heterozygous for the candidate rSNP to 0.

When the rSNP is not in $r^2 \sim 1$ with the daeSNP, the distribution of the AE ratios will depend on the rSNP-daeSNP haplotypes present in the analysed samples. In this scenario we applied, we applied a two-sample Wilcox test for the null hypothesis that the absolute AE ratios at the samples heterozygous for the candidate rSNP are higher than the absolute AE ratios at the samples homozygous for the tested rSNP. These tests were performed for rSNP-daeSNP pairs located within 500 kb of each other. p-values were adjusted with the Benjamini−Hochberg method[28], using all daeSNP/tested SNP pairs, with the distance between them as a covariate (package ihw, R)[29] and reported as significant when the false discovery rate was below 5%.

Breast cancer GWAS data retrieval

One thousand and eleven GWAS-significant risk-associated SNPs for BC published until April 2018 were retrieved from the NHGRI-EBI Catalog of published genome-wide association studies (GWAS Catalog)[30] using the gwasrapidd R package[31]. We applied a suggestive p-value threshold (p ≤ 1.0E−05) to capture a broader set of potentially significant variants, including those identified in meta-analyses and replication studies, to ensure the inclusion of biologically relevant findings. This approach aimed to provide a comprehensive and robust analysis. Additionally, we included only studies involving European populations and the following reported traits: "Breast cancer", "Breast cancer (early onset)", "Breast cancer (estrogen-receptor negative)", "Breast cancer (male)", "Breast cancer in BRCA1 mutation carriers", "Breast cancer in BRCA2 mutation carriers", "Breast cancer male", and "Breast cancer and/or colorectal cancer". The complete list of SNPs is presented in Table S1.

Proxy SNP retrieval

Variants in LD with index SNPs were retrieved from Ensembl[32] using the function get_ld_variants_by_window() from the ensemblr R package (https://github.com/ramiromagno/ensemblr) using the 1000 GENOMES project data (phase_3) for the CEU population and a genomic window size of 500 kb (250 kb upstream and downstream of the queried variant). The r^2 cut-off used varied between 0.2 and 0.95 depending on the analysis and is indicated in each analysis description.

Annotation of variants

Variants were annotated according to hg38/GRCh38 with biomaRt v 2.40.5. aeSNP consequence types were categorised as follows: UTR if classified as 3_prime_UTR_variant or 5_prime_UTR_variant; coding if classified as coding_sequence_variant, incomplete_terminal_codon_variant, missense_variant, stop_retained_variant, synonymous_variant, stop_lost, start_lost, stop_gained, splice_region_variant, splice_acceptor_variant or splice_donor_variant; intronic if classified as intron_variant; and noncoding_transcript_variant if classified as noncoding_transcript_variant, noncoding_transcript_exon_variant or mature_miRNA_variant. We classified aeSNPs further according to gene biotype as follows: pseudogene if located in IG_C_pseudogene, processed_pseudogene, transcribed_unprocessed_pseudogene, transcribed_unitary_pseudogene, translated_unprocessed_pseudogene, unprocessed_pseudogene, unitary_pseudogene, transcribed_processed_pseudogene, polymorphic_pseudogene or rRNA_pseudogene; protein-coding gene if located in protein_coding, IG_V_gene, TR_C_gene, TR_J_gene, TR_V_gene or TEC; and noncoding_rna if located in lncRNA, miRNA, misc_RNA, snRNA, snoRNA, scaRNA or ribozyme.

To test whether classes of consequence type and gene biotype were overrepresented (i.e., enriched) in the list of daeSNPs, we applied two-tailed Fisher's exact tests. Information from imprinted genes was retrieved from a comprehensive study of genomic imprinting in the breast[33] and from the geneimprint database (http://www.geneimprint.com) searching for Imprinted Genes: by Species: Human.

Retrieval of previously suggested BC target genes

Genes previously suggested as targets of cis-acting regulatory variation in post-GWAS studies for BC, with extensive fine-scale mapping and in silico prediction or functional analysis, and those classified as *Inquisit 1* by Fachal et al.[4] are indicated in Table S2.

GTEx eQTL and gene expression data retrieval

The Genotype-Tissue Expression (GTEx) project identified expression quantitative trait loci (eQTL) using normal mammary tissue samples[34]. eGenes (genes with at least one SNP in cis significantly associated, at a false discovery rate (FDR) of ≤ 0.05, with expression differences of that gene) and significant variant-gene associations based on permutations were downloaded from GTEx Analysis V8 (dbGaP Accession phs000424.v8.p2, available on 18/07/2019).

All SNP-gene associations tested for breast mammary tissue, including nonsignificant and gene expression levels (TPM), were downloaded from GTEx Analysis V7 (available on 2016-01-15).

Comparison of daeGenes, eGenes and gwasGenes

First, the list of publicly available eGenes was compared with the daeGenes identified in our study, restricting this comparison to genes analysed in both datasets. Then, we investigated the percentage of gwasGenes, defined as genes containing variants in moderate to strong LD ($r^2 \geq 0.4$) with GWAS index SNPs, displaying evidence of cis-regulation by either DAE or eQTL analysis.

Functional characterisation of candidate risk SNPs

daeQTLs in moderate to strong linkage disequilibrium (LD) ($r^2 \geq 0.4$) with GWAS index SNPs were defined as risk-daeQTLs. These variants, along with their proxies ($r^2 \geq 0.95$), were considered candidate risk rSNPs in the subsequent analysis. Candidate risk rSNPs were examined for regulatory potential by assessing the overlap of the variant's location with epigenetic marks derived from the ENCODE[35] and NIH Roadmap Epigenomics project data[36] using the R package haploR (https://github.com/cran/haploR). Candidate causal variants (variants overlapping with DNase I hypersensitivity sites and H3K4me1 or H3K4me3 or histone modifications in normal breast or breast tumour cell lines) at the 5q14.1–14.2 locus were further analysed regarding their genomic context and transcription factor (TF) binding using the UCSC Genome Browser[37,38], HaploReg v4.1[39] and RegulomeDB v1.1[40] tools. Emphasis was given to overlapping with transcription factor (TF) binding identified in breast myoepithelial cells (BR. MYO, E027), human mammary epithelial cells (HMECs, E119), variant human mammary epithelial cells (vHMECs, E028) and two BC cell lines (MCF-7 and T47D). Allele-specific epigenetic modifications (H3k4me3 and DNase I), RNA polymerase II (POL2) and transcription factors (TF) binding with alignment data available in HMEC, MCF-7 and MCF-10A breast cancer cell lines from ENCODE were retrieved and visualised using the Integrative Genomics Viewer (IGV Version 2.3.71) tool[41], to analyse protein−DNA interactions and allelic preferential binding. Differential allelic binding was analysed in heterozygous candidate risk rSNPs located within TF binding peaks in experiments with a read coverage at the SNP site ≥ 20. We applied a two-tailed binomial test with the null hypothesis assuming no bias (balanced binding of the protein to the two alleles of the variant). The p-value was corrected for multiple testing using the R package qvalue[42]. When multiple tracks for the same SNP, trait and cell line existed, only the p-value for the experiment with higher total read counts was reported in the main manuscript.

Analysis related to alternative transcription at the 5q14.1–14.2 locus was carried out in three ways. First, sQTLseekeR (v1.4)[43] was used to test the association of genetic variants with alternative isoform expression in both normal breast and tumour tissue using total read counts derived from RNA-seq data from the TCGA (TCGA-BRCA, hg19) and GTEx (phs000424.v6.p1, hg38) projects. Only *ATG10* displayed sufficient alternative transcription dispersion to allow sQTL analysis. Additionally, all SNPs within 5 kb upstream or downstream of *ATG10* were included in the analysis, not only the candidate risk rSNPs, to increase the stringency of the association exercise. P-values for all SNPs tested for ATG10 sQTL analysis were controlled for multiple testing using a 5% FDR. Correlation analyses between -log10 (FDR q-value) and LD (r^2) with rs7707921 were performed using Pearson's test. Then, the overlapping of variant location with RNA processing-associated proteins was assessed

using CLIP data retrieved from POSTAR2 (http://lulab.life.tsinghua.edu.cn/postar/)[44] and from RBP-Var (http://www.rbp-var.biols.ac.cn/)[45], which additionally informed on riboSNitch potential[46]. Finally, allele-specific RBP binding predictions were performed with RBPmap[47] using the analysed variant flanking sequence (30 nucleotides on each side, with the variant at index 31) using all available human RBP motifs.

Haplotype analysis

Haplotypes in the 5q14.1–14.2 region were analysed on Haploview 4.2 using the imputed genotypes from the 64 normal breast tissue samples[48]. For candidate risk SNPs whose genotype was not possible to determine (because it was neither genotyped nor imputed), a proxy SNP in strong LD ($r^2 \geq 0.95$) was used instead. Haplotype blocks were generated using the default algorithm.

TCGA-BRCA gene expression analysis

Processed gene expression and isoform expression from RNA-Seq data for 113 normal solid tissues and 1102 primary solid tumours from the TCGA-BRCA project, together with corresponding clinical data, were retrieved from the Genomic Data Commons archive using the R package TCGAbiolinks[49] accessed in October 2018. Isoform expression was annotated according to the genome assembly hg19, and total gene expression was annotated according to hg38. We applied two-sample Wilcoxon tests to compare the mean expression of *ATG10* isoforms between normal-solid tissues (normal-matched) and breast tumours, correcting for multiple testing with the Benjamini and Hochberg (BH) procedure. We applied Pearson's test to correlate gene expression among *ATG10*, *RPS23*, and *ATP6AP1L*. Spearman's test was applied to correlate *ATG10*, *RPS23*, and *ATP6AP1L* with *MYC* and *MAX* gene expression.

Results

Cis-regulatory variation is common in normal breast tissue

Genome-wide allelic expression (AE) analysis was performed using microarray data from 64 normal breast tissue samples. Of these, 61 samples were of European ancestry (EUR), two samples were of American ancestry (AMR) and one sample was of African ancestry (AFR) (Fig. S2). Normalised allelic expression ratios were calculated for SNPs in coding and noncoding regions upon filtering for the cDNA signals' expression level and allelic discrimination potential. Overall, we identified 91,467 autosomal allelic-expressed SNPs (aeSNPs) located in 21,527 annotated Ensembl genes (median of three aeSNPs per gene) (Fig. S3). Unsurprisingly, the number of aeSNPs analysed per gene correlated with the annotated gene length (rho = 0.60, p-value < 2.2e−16, Fig. S4).

We found that almost one-third of the aeSNPs (26,266 out of 91,467) displayed biallelic differential expression (daeSNPs, q-value ≤ 0.05) (Table 1, Table S3), while 84 SNPs displayed monoallelic expression (maeSNPs). TaqMan PCR validated seven out of nine daeSNPs (Fig. S5) that showed significant DAE and concordant preferential expression (Fisher's exact test p-value > 0.05).

The daeSNPs are distributed across the genome, with low interchromosomal variability (ranging from 26 to 35%, Fig. S6). They overlapped 13,688 (65%) annotated genes (daeGenes), of which 3666 (17%) harboured three or more daeSNPs (Fig. 2a, Table 1, Table S3). When considering daeSNPs mapping exclusively to one gene, we identified 8193 daeGenes (out of 12,944) that showed evidence of being under the control of allele-specific cis-acting factors, either genetic or epigenetic. In terms of consistency of DAE detection across the length of these genes, we found that in the majority of daeGenes, the frequency of daeSNPs was higher than 40% (7476 in 13,688), with 3894 daeGenes presenting imbalances in all the analysed aeSNPs (Fig. 2b). The aeSNPs showed a large distribution of mean |AE ratios|, with daeSNPs centred at 0.60 (corresponding to a difference between alleles of 1.5) and non-daeSNPs centred at 0.26 (corresponding to a difference of 1.2). Twelve per cent of daeSNPs showed average absolute AE ratios between 1 and 5, corresponding to average allelic fold changes ranging from 2 to 34 (Fig. 2c, Table S3). The amplitude of the imbalances measured at aeSNPs correlated negatively with the average expression level of both alleles (rho = −0.4, p-value < 2.2e−16) (Fig. 2d) but not with the standard deviation across individuals (Fig. S7). The aeSNPs are located mainly in intronic regions and noncoding transcript genes, but non-daeSNPs and daeSNPs showed differences in class distribution for consequence type, with daeSNPs enriched at unannotated regions and depleted at intronic, non-coding regions and UTRs (p-value < 0.05, Fig. 2e). Although most of the aeSNPs analysed were in protein-coding genes, daeSNPs were relatively more common in noncoding genes and pseudogenes when compared to non-daeSNPs and depleted in protein-coding genes (p-value < 0.05, Fig. 2f).

Monoallelic expression in breast tissue

Regarding monoallelic expression, maeSNPs were annotated to 44 Ensembl genes (Table 1, Table S4, Fig. S8), the majority of which were previously reported as imprinted in breast tissue (e.g., *IGF2* or *ZDBF2*) or in other tissues (e.g., *KCNQ1*, *KCNQ1OT1*, *RTL1*, *NAA60*, *ZIM2,* and *L3MBTL1*), validating our AE analysis. Interestingly,

Set of SNPs	n	Ensembl gene IDs
All aeSNPs	91,467	21,527
maeSNPs	84	44
daeSNPs	26,266	13,689

Table 1. Summary of the genome-wide breast tissue allelic expression analysis results.

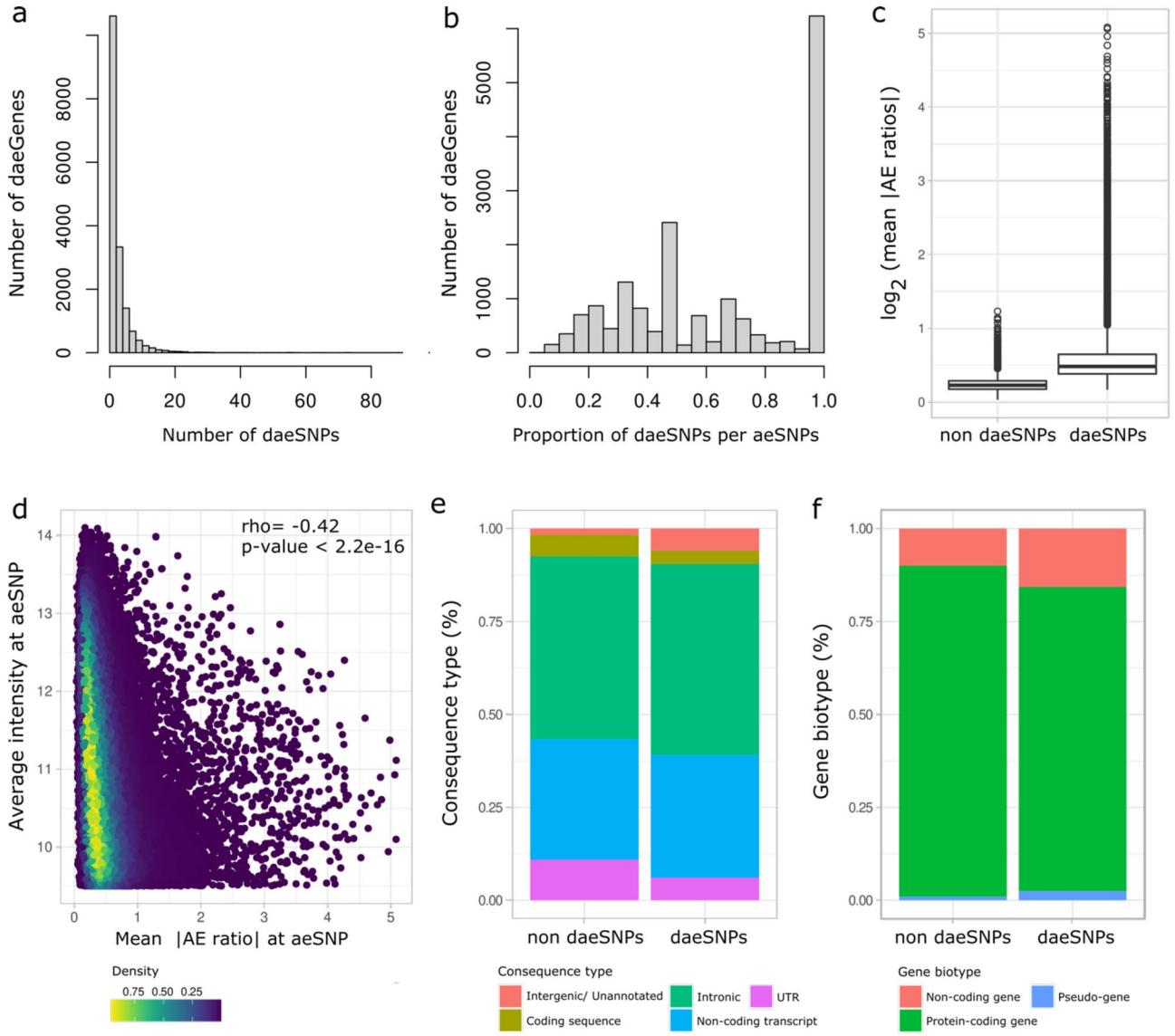

Fig. 2. Characterisation of aeSNPs. (**a**) Histogram of the rank number of daeSNPs identified per gene across 17,135 annotated genes. (**b**) Histogram of the rank proportion of daeSNPs per aeSNPs identified per gene. (**c**) Box plot with the distribution of the mean of the absolute values of AE ratios across heterozygous individuals measured at non-daeSNPs and daeSNPs. (d) Distribution of the mean absolute values of AE ratios at aeSNPs according to the average intensity of both alleles at aeSNPs in the microarray Spearman's results of a Spearman's correlation test are shown. (**e,f**) Relative frequency of aeSNPs and daeSNPs according to consequence type and gene biotype, respectively.

we detected maeSNPs in a region containing the lncRNA *MEG9* and a cluster of miRNA genes that had only previously been reported as imprinted in nonhuman species[50–52]. Additionally, we found unreported monoallelic expression at an intergenic region (22q11.23), suggesting the existence of unannotated transcripts in this region. Notably, we observed two groups of heterozygotes preferentially expressing opposite alleles of rs17122278, an intronic variant of *ARCN1*, suggesting the latter as a candidate novel monoallelically expressed protein-coding gene in breast tissue.

Mapping of daeQTLs in normal breast tissue

Evidence of DAE supports that a gene's expression is controlled by cis-regulatory variation, which can be mapped using AE ratios as a quantitative trait—in what we termed DAE quantitative trait loci (daeQTL) analysis. Here, we found a minority of daeSNPs (6928 out of 26,266) for which all the heterozygotes preferentially expressed the same allele. This pattern indicates moderate to strong linkage disequilibrium between the daeSNP and the rSNPs acting on it[27]. Hence, our mapping approach considered the allelic expression (AE) ratio distribution pattern displayed at each daeSNP, and one-sample or two-sample Wilcox tests were applied accordingly. We identified 54,357 daeQTLs (5% FDR) for 6761 (26%) daeGenes (Table S5), primarily located within 20 kb from the corresponding daeSNP but as far as the 500 kb window used for the analysis (Fig. 3a). daeQTLs for *MROH8*

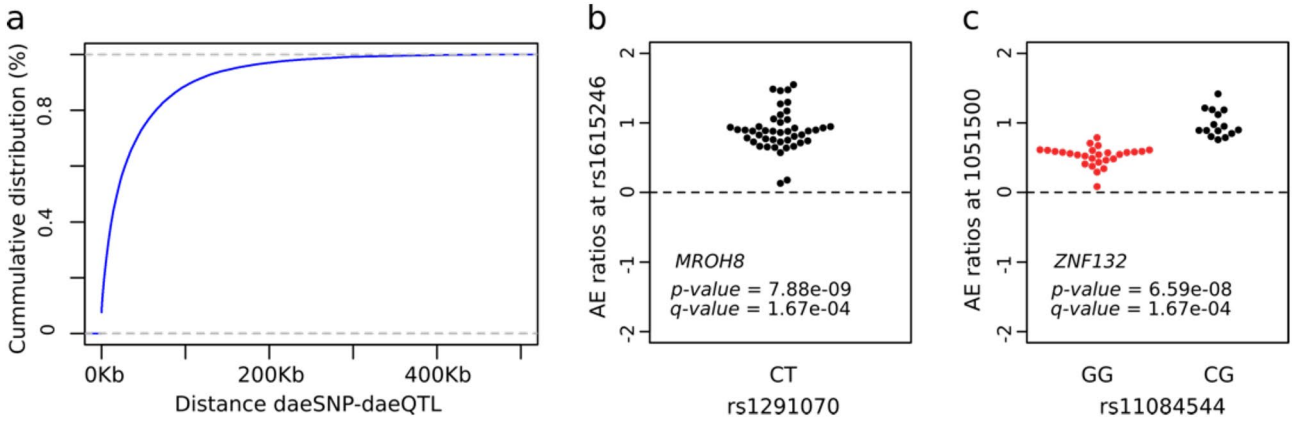

Fig. 3. Mapping of variants associated with differential allelic expression. (**a**) Empirical cumulative distribution for the distance between the daeSNP and corresponding mapped daeQTL. (**b,c**) daeQTL mapping result for the most significant daeQTL identified for *MROH8* using a one-sample Wilcox test and for *ZNF132* using a two-sample Wilcox test. The AE ratios calculated at the daeSNPs are represented on the y-axis in the two panels and stratified according to genotype at the candidate SNP (black dots represent heterozygous individuals, and red dots represent homozygous individuals).

and ZNF132, two coding genes located on chromosomes 19 and 20, respectively, were among the most significant ones found (Fig. 3b,c), but we identified other highly significant daeQTLs (adjusted p-values smaller than 5.0E−04) for 2507 genes.

Identification of target genes within BC risk loci

To pinpoint the most likely candidate target genes within BC risk loci, a main post-GWAS challenge, we identified the genes within previously reported GWAS loci (gwasGenes) displaying the most robust evidence of being under the control of cis-regulatory variation, provided either by DAE (daeGenes) or eQTL (eGenes) analysis. We found that most gwasGenes (783 out of 948) showed such evidence, with 69% of these with evidence via DAE analysis (358 genes identified solely by DAE and 300 by both analyses) (Table S6). Compared to all genes studied, gwasGenes presented a significant enrichment of Fisher's significance of DAE (Fisher's exact test = 2.48e−05). Finally, we successfully mapped daeQTLs for 385 gwasGenes (Fig. 4, Table S6).

Next, we verified our ability to identify 178 previously proposed breast cancer target genes (Table S2). We found that 44% of these genes were exclusively daeGenes (e.g., *ELL, TOX3,* RNF115), 23% were both daeGenes and eGenes (e.g., *CASP8, POU5F1B, STXBP4*) and 14% were exclusively eGenes (e.g., *RMND1, HELQ, PRKRIP1*). However, we did not find evidence supporting other genes, such as C*ITED4, IGFBP5 and MYC.* (Table S2). As total levels of gene expression may confound the ability to identify daeGenes and eGenes, it is noteworthy that eGenes showed higher median levels overall than daeGenes, and only 4.7% of exclusive daeGenes showed low median levels (< 0.1 TPM) (Fig. S9).

Identification of causal variants within BC risk loci

Another post-GWAS challenge we addressed was the identification of the causal variants within risk loci. We first identified 1416 daeQTLs in moderate to strong LD ($r^2 \geq 0.4$) with GWAS index SNPs (Fig. 1) (GWAS p-value < 1.0E−05), henceforth referred to as risk-daeQTLs. These were distributed across 93 loci in 19 chromosomes, primarily in introns, followed by intergenic regions (Table S7, Fig. S10). Then, we assessed these risk-daeQTLs plus their proxies ($r^2 \geq 0.95$) for their cis-acting regulatory potential. We started by identifying 425 variants located in DNase I hypersensitivity sites (DHS), of which the majority (69%) mapped to regions with histone marks associated with active regulatory elements (Fig. 4b, Fig. S11). More specifically, 149 risk-daeQTLs localised in both active promoter (H3K4me3 and H3K9ac) and regions with active enhancer-associated (H3K4me1 and H3K27ac) histone marks, 76 localised exclusively in regions with active enhancer-associated marks and another 67 exclusively localised in regions with active promoter-associated marks. Of these, 122 risk-daeQTLs also showed protein binding evidence, thus representing strong candidate causal variants within 41 of the initial 93 BC risk loci (Table S8).

Among these 41 risk loci, we detected 47 novel candidate target genes in 29 loci with no previous report of target genes, such as *SMC2* in 9q31.1, *MLLT10* in 10p12.32 and *MAN2C1* and *PTPN9* in 15q24.2. We confirmed previously reported target genes in nine loci and identified eight novel genes, including *NASP* and *IPP* in 1p34.1 and *ATP6AP1L* in 5q14.1. Finally, we identified strong candidate causal variants at three loci but could not discern the target gene due to a lack of genomic annotation (Table 2, Table S9).

Notably, 2222 daeQTLs were also in lower LD with GWAS hits ($0.2 \leq r^2 < 0.4$), representing a valuable dataset warranting further exploration (Table S10).

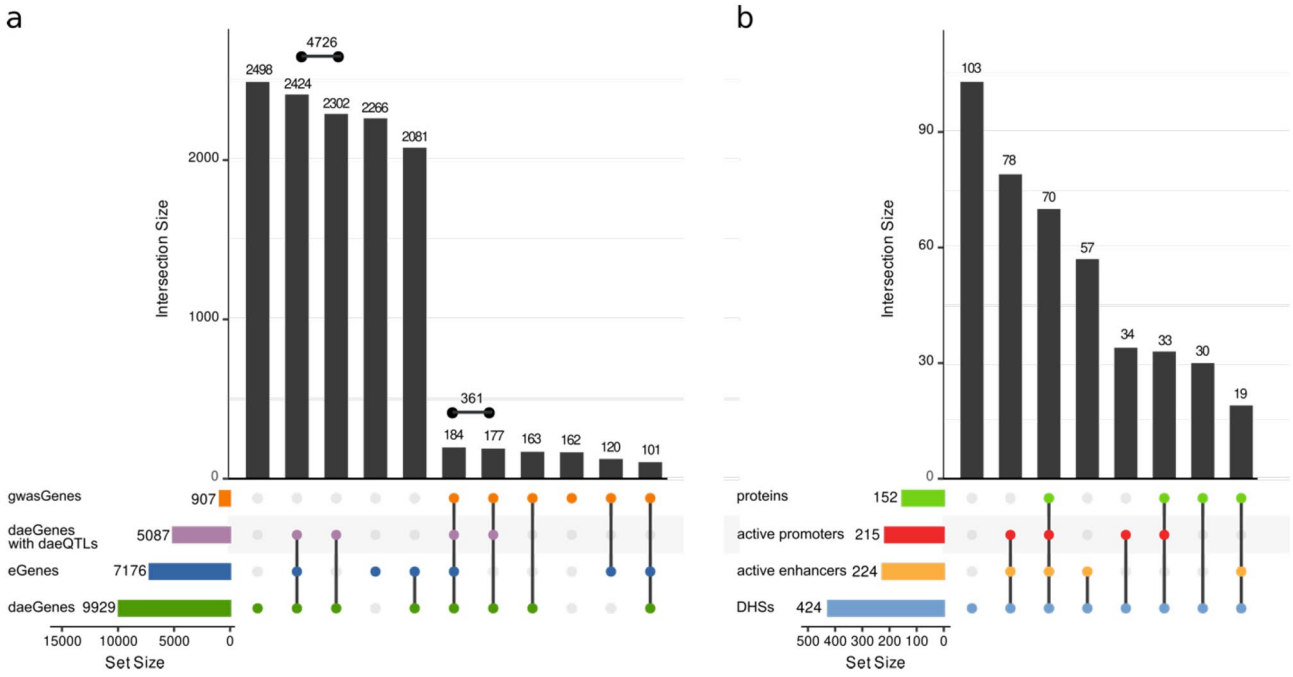

Fig. 4. Summary of colocalisation analyses for daeGenes and risk-daeQTLs. (**a**) UpSet plot for 15,706 genes tested for DAE and eQTL (GTEx breast mammary tissue). *daeGenes* genes identified as having differential allelic expression in normal breast tissue; *eGenes* genes reported as being eQTL genes in GTEx mammary tissue data (q-value ≤ 0.05); *gwasGenes* genes where GWAS index SNPs or proxies ($r^2 \geq 0.4$) are located, *daeGenes with daeQTL mapping* daeGenes for which daeQTLs were identified. (**b**) UpSet plot for 424 variants located in DHSs, according to the presence of protein binding and location in active promoters and/or enhancers in breast cell lines.

Mapping of cis-regulatory risk variants at the 5q14.1–14.2 locus

To further show the potential use of our integrated approach, we focused our follow-up studies on the BC risk locus 5q14.1–14.2, where some of the most significant risk-daeQTLs and candidate causal variants were identified. In this locus, rs7707921 was previously associated with BC risk in two meta-analyses (OR for alternative A allele = 1.07, 95% CI [1.05–1.1], p = 5E−11)[9,53]. The region containing this intronic variant of *ATG10*, its proxy variants ($r^2 \geq 0.4$) and other risk-associated variants reported in this locus spans three genes (*ATG10*, *RPS23*, and *ATP6AP1L*), hindering the identification of the causal variant(s) and their target gene(s) in this locus.

First, all three genes showed DAE, supporting their regulation by cis-regulatory variants: 10 daeSNPs out of 37 aeSNPs at *ATG10*, one daeSNP out of two aeSNPs at *RPS23* and three daeSNPs out of five aeSNPs at *ATP6AP1L* (Fig. S12). The highest mean |AE ratios| detected at daeSNPs in these genes was 1.27 (2.4-fold) at *RPS23*, followed by 0.92 (1.9-fold) at *ATP6AP1L* (Fig. 5—panel 2, Fig. S11). By daeQTL mapping analysis, we identified daeQTLs for all three genes: 56 for *ATG10 (*spreading along the *ATG10-ATP6AP1L* region), 4 for *RPS23 (*limited *to RPS23-ATP6AP1L)* and 26 for *ATP6AP1L (*spreading along the *ATG10-ATP6AP1L* region) (Fig. 5—panels 3 to 5). Additionally, we classified as risk-daeQTLs the 38 *ATG10* daeQTLs and 24 *ATP6AP1L* daeQTLs (22 of which are common to the two genes) in moderate to strong LD ($r^2 \geq 0.4$) with the risk-associated variants. Furthermore, both *ATG10* and *ATP6AP1L* daeQTL analysis results strongly correlated with the corresponding LD with the GWAS lead-SNP rs7707921 (Fig. S13), further supporting the role of variants regulating the expression of these two genes in the risk for breast cancer.

Cis-regulatory risk variants act via two different mechanisms on genes in the 5q14.1–14.2 locus

The overlap analysis of the risk-daeQTLs with epigenetic marks in breast cell lines identified seven candidate causal variants for *ATG10* and *ATP6AP1L* (Tables S8, S11). We investigated these variants further for allelic differences in transcription factor binding and association with histone modifications and DHSs. One of these SNPs, rs111549985, overlies the active promoter of *ATG10* (Fig. S14), and its minor G-allele is preferentially associated with the H3K4Me3 modification in HMECs (2.7-fold, p = 3.7e−03) and shows robust preferential binding by POL2 in MCF7 cells (ninefold, $p = 4.0E{-}04$). However, DHS was more significantly associated with the major/reference C allele in T47D cells (0.5-fold, $p = 4.6e{-}05$) (Fig. 6a, Table S12). Another two candidate causal variants, rs226198 (intronic to *RPS23*) and rs688025′ UTR (located at *RPS23* 5′ UTR), overlay the shared promoter of *RPS23* and *ATP6AP1L* and a predicted enhancer interacting with the *ATG10* promoter (Fig. S15). The minor C-allele of rs226198 showed preferential binding by MYC and MAX transcription factors, which are known to cooperate in cancer[54] (12.6-fold and 7.9-fold difference, respectively, $p < 2.2e{-}16$) and preferential H3K4me3 marking (2.7-fold, $p = 1.4e{-}02$) in MCF-7 cells (Fig. 6b, Table S12). It would be interesting to elucidate whether

Chr_band	GWAS variant	GWAS nearest gene	Candidate causal variants	daeQTL gene	Regulatory feature
A. Loci with novel suggested target genes					
1p36.23	rs225132	ERRFI1-DT	rs12757968	ERRFI1-DT	Active enhancer
1q22	rs10796944, rs7524950	ASH1L, PKLR	rs1046188	FDPS, RUSC1-AS1	Active promoter and active enhancer
1q22	rs348196, rs10796944, rs12091730, rs7524950	DAP3, ASH1L, MSTO1, DAP3P1, PKLR	rs2048431	FDPS, RUSC1-AS1	Active promoter and active enhancer
1q22	rs348196	DAP3	rs3841838	ARHGEF2, RIT1	Active promoter and active enhancer
1p23.2	rs67073037	WDR43	rs4407214	WDR43	Active promoter and active enhancer
4p12	rs199501877	NIPAL1, TXK	rs98270	NIPAL1	Active promoter and active enhancer
5q11.1	rs145106188	EMB	rs4865698	EMB	Active enhancer
5q11.1	rs145106188	EMB	rs4865699	EMB	Active enhancer
5q11.1	rs145106188	EMB	rs28528780	EMB	Active promoter and active enhancer
5q31.1	rs6860806	SLC22A4	rs1979981	SLC22A4, MIR3936HG, SLC22A5	Active promoter and active enhancer
5q31.1	rs6860806	SLC22A4	rs162887	SLC22A4, MIR3936HG, SLC22A5	Active promoter and active enhancer
5q31.1	rs6860806	SLC22A4	rs460089	SLC22A4, MIR3936HG, SLC22A5	Active promoter and active enhancer
5q31.1	rs6860806	SLC22A4	rs460271	SLC22A4, MIR3936HG, SLC22A5	Active promoter and active enhancer
5q31.1	rs6860806	SLC22A4	rs367805	SLC22A4, MIR3936HG, SLC22A5	Active enhancer
5q31.1	rs6860806	SLC22A4	rs2631369	SLC22A4, MIR3936HG, SLC22A5	Active promoter and active enhancer
5q31.1	rs6860806	SLC22A4	rs2631368	SLC22A4, MIR3936HG, SLC22A5	Active promoter and active enhancer
5q31.1	rs736801	ENSG00000283782	rs2070721	ENSG00000283782	Active promoter and active enhancer
5q31.1	rs736801	ENSG00000283782	rs2548998	ENSG00000283782	Active promoter and active enhancer
6p22.2	rs17598658, rs13195401	H2BC6, BTN2A1	rs9467701	BTN3A2	Active promoter and active enhancer
6p22.2	rs17598658, rs13195401	H2BC6, BTN2A1	rs6923139	BTN3A2	Active promoter and active enhancer
6p22.2	rs17598658, rs13195401	H2BC6, BTN2A1	rs6903015	BTN3A2	Active promoter and active enhancer
6p22.2	rs17598658, rs13195401	H2BC6, BTN2A1	rs68112369	BTN3A2	Active promoter
6p22.2	rs17598658, rs13195401	H2BC6, BTN2A1	rs66827971	BTN3A2	Active promoter
6p22.2	rs13195401	BTN2A1	rs9379873	BTN3A2	Active promoter and active enhancer
6p22.2	rs71557345, rs13195401	ENSG00000285571, BTN2A1	rs36162392	BTN3A2	Active promoter and active enhancer
6p22.1	rs3094146, rs1611579	ZNRD1ASP, ENSG00000285799	rs707910	HLA-A	Active promoter and active enhancer
6p22.1	rs3094146, rs1611579	ZNRD1ASP, ENSG00000285799	rs415137	HLA-A	Active promoter and active enhancer
6p22.1	rs3094146, rs1611579	ZNRD1ASP, ENSG00000285799	rs438610	HLA-A	Active promoter and active enhancer
6p22.1	rs3094054, rs3094146, rs3132615	UBQLN1P1, ZNRD1ASP, ENSG00000288805	rs2188100	HCG17, HLA-L	Active promoter and active enhancer
6p22.1	rs3129984, rs3132610, rs9262142, rs3132615	ENSG00000288805, HCG20, ABCF1, PPP1R18	rs9262142	C6orf136	Active promoter and active enhancer
7q21.3	rs847577	LMTK2	rs1874343	TECPR1	Active promoter and active enhancer
9q31.1	rs4742903, rs718857	SMC2	rs3818625	SMC2	Active promoter
9q31.1	rs4742903, rs718857	SMC2	rs3818626	SMC2	Active promoter
9q31.1	rs4742903, rs718857	SMC2	rs10820599	SMC2	Active promoter
9q31.1	rs4742903, rs718857	SMC2	rs10820600	SMC2	Active promoter
9q31.1	rs4742903, rs718857	SMC2	rs4742903	SMC2	Active promoter
10p12.31	rs7072776, rs10828247, rs11012730, rs10828249, rs7098100	MLLT10, SKIDA1	rs10828247	MLLT10	Active promoter

Continued

Chr_band	GWAS variant	GWAS nearest gene	Candidate causal variants	daeQTL gene	Regulatory feature
10p12.1	rs7918232	ANKRD26	rs7907988	YME1L1	Active promoter and active enhancer
10q21.2	rs10822013	ENSG00000285837, ZNF365	rs10822013	ENSG00000285837	Active enhancer
11p11.2	rs11039183	MADD	rs7947450	SPI1	Active promoter
11q13.1	rs617791	DRAP1, TSGA10IP	rs14157	SART1	Active promoter
11q13.1	rs617791	DRAP1, TSGA10IP	rs12794370	SART1	Active promoter and active enhancer
11q13.2	rs1783730	TMEM151A	rs33981819	ENSG00000254458	Active promoter and active enhancer
11q13.2	rs11344495, rs55908905	CTSF, SPTBN2	rs11110	DPP3-DT, B4GAT1-DT	Active promoter and active enhancer
11q13.2	rs11344495, rs55908905	CTSF, SPTBN2	rs55853079	DPP3-DT, B4GAT1-DT	Active promoter and active enhancer
11q22.3	rs11374964	POGLUT3	rs228589	NPAT	Active promoter
11q22.3	rs11374964	POGLUT3	rs189037	NPAT	Active promoter
11q23.1	rs505372	SIK2	rs541198	NA	Active promoter and active enhancer
11q23.1	rs505372	SIK2	rs7107213	CRYAB	Active promoter and active enhancer
14q13.2	rs58327846	PRORP	rs1056879	PRORP	Active promoter and active enhancer
14q13.2	rs58327846	PRORP	rs2236167	PRORP	Active promoter and active enhancer
14q32.33	rs60226654	COA8	rs3759586	KLC1, XRCC3	Active enhancer
15q21.1	rs1876206	FBN1	rs8029993	FBN1	Active enhancer
15q24.2	rs60381548, rs8027365	SIN3A, PTPN9	rs11637068	MAN2C1, PTPN9	Active promoter and active enhancer
15q24.2	rs60381548, rs8027365	SIN3A, PTPN9	rs75219778	MAN2C1, PTPN9	Active promoter
15q24.2	rs60381548, rs8027365	SIN3A, PTPN9	rs62027209	MAN2C1, PTPN9	Active promoter and active enhancer
15q26.1	rs77554484	PRC1, ENSG00000284946	rs867468	PRC1, PRC1-AS1, ENSG00000284946	Active promoter and active enhancer
15q26.1	rs77554484	PRC1, ENSG00000284946	rs2001216	PRC1, PRC1-AS1, ENSG00000284946	Active promoter and active enhancer
15q26.1	rs77554484	PRC1, ENSG00000284946	rs12905855	PRC1, PRC1-AS1, ENSG00000284946	Active promoter and active enhancer
16q12.2	rs17817449, rs62033406, rs7193144, rs62048402	FTO	rs9940128	FTO	Active enhancer
16q12.2	rs17817449, rs62033406, rs7193144, rs62048402	FTO	rs11642015	FTO	Active enhancer
16q12.2	rs17817449, rs62033406, rs7193144, rs62048402	FTO	rs17817497	FTO	Active enhancer
16q12.2	rs17817449, rs62033406, rs7193144, rs62048402	FTO	rs8050136	FTO	Active enhancer
16q13	rs2303282, rs2432539	BBS2, AMFR	rs2440467	AMFR	Active enhancer
17q21.31	rs2732699	ARL17B	rs76594404	CRHR1, KANSL1, LINC02210, LINC02210-CRHR1, MAPT, MAPT-AS1, ARL17B	Active promoter and active enhancer
17q21.31	rs2732699	ARL17B	rs80233201	CRHR1, KANSL1, LINC02210, LINC02210-CRHR1, MAPT, MAPT-AS1, ARL17B	Active promoter and active enhancer
17q21.31	rs2732699	ARL17B	rs62056778	CRHR1, KANSL1, LINC02210, LINC02210-CRHR1, MAPT, MAPT-AS1, ARL17B	Active promoter and active enhancer
17q21.31	rs2732699	ARL17B	rs11575895	CRHR1, KANSL1, LINC02210, LINC02210-CRHR1, MAPT, MAPT-AS1, ARL17B	Active promoter
17q21.31	rs2732699	ARL17B	rs62056779	CRHR1, KANSL1, LINC02210, LINC02210-CRHR1, MAPT, MAPT-AS1, ARL17B	Active promoter
17q21.31	rs2732699	ARL17B	rs74548327	CRHR1, KANSL1, LINC02210, LINC02210-CRHR1, MAPT, MAPT-AS1, ARL17B	Active promoter
17q21.31	rs2732699	ARL17B	rs111972148	CRHR1, KANSL1, LINC02210, LINC02210-CRHR1, MAPT, MAPT-AS1, ARL17B	Active promoter
17q21.31	rs2732699	ARL17B	rs242561	CRHR1, KANSL1, LINC02210, LINC02210-CRHR1, MAPT, MAPT-AS1, ARL17B	Active promoter

Continued

Chr_band	GWAS variant	GWAS nearest gene	Candidate causal variants	daeQTL gene	Regulatory feature
17q21.31	rs2732699	ARL17B	rs2316951	CRHR1, KANSL1, LINC02210, LINC02210-CRHR1, MAPT, MAPT-AS1, ARL17B	Active enhancer
17q21.31	rs2732699	ARL17B	rs11079733	CRHR1, KANSL1, LINC02210, LINC02210-CRHR1, MAPT, MAPT-AS1, ARL17B	Active promoter
17q21.31	rs2732699	ARL17B	rs2696633	CRHR1, KANSL1, LINC02210, LINC02210-CRHR1, MAPT, MAPT-AS1, ARL17B	Active promoter
17q21.31	rs2732699	ARL17B	rs143625699	ARL17B, KANSL1	Active promoter
17q21.31	rs2732699	ARL17B	rs113417378	CRHR1, KANSL1, LINC02210, LINC02210-CRHR1, MAPT, MAPT-AS1, ARL17B	Active promoter
17q21.31	rs2732699	ARL17B	rs143191191	CRHR1, KANSL1, LINC02210, LINC02210-CRHR1, MAPT, MAPT-AS1, ARL17B	Active enhancer
22q13.31	rs28512361	ENSG00000235091	rs134847	ATXN10	Active promoter
22q13.31	rs28512361	ENSG00000235091	rs2071872	ATXN10	Active promoter and active enhancer
B. Loci with previously suggested target genes					
1p34.1	rs12077974	MAST2	rs6697821	NASP#, IPP#	Active promoter and active enhancer
1p34.1	rs12077974, rs1707302	MAST2, PIK3R3	rs1707303	NASP#, IPP#, PIK3R3	Active promoter and active enhancer
1p34.1	rs12077974	MAST2	rs1707302	NASP#, IPP#, PIK3R3	Active enhancer
2q33.1	rs10931936, rs1035142, rs1830298, rs700635, rs3769821	CASP8	rs3769823	CASP8	Active promoter and active enhancer
3q12.1	rs9837602, rs9833888, rs9289981	CMSS1, FILIP1L	rs793463	CMSS1#, FILIP1L	Active enhancer
3q12.1	rs9837602, rs9833888	CMSS1, FILIP1L	rs28714363	CMSS1#, FILIP1L	Active enhancer
5q14.1	rs7707921, rs111549985, rs2407064, rs146817970, rs2407156	ATG10, ATP6AP1L	rs111549985	ATG10, ATP6AP1L	Active promoter and active enhancer
5q14.1	rs7707921, rs2407064, rs146817970, rs2407156	ATG10	rs226198	ATG10, ATP6AP1L	Active promoter and active enhancer
5q14.1	rs7707921, rs2407064, rs146817970, rs2407156	ATG10	rs6880209	ATG10, ATP6AP1L	Active promoter and active enhancer
5q14.1	rs7707921, rs2407064, rs146817970, rs2407156	ATG10	rs11325430	ATG10, ATP6AP1L	Active promoter and active enhancer
5q14.1	rs7707921, rs2407064, rs146817970	ATG10	rs17247678	ATG10, ATP6AP1L	Active enhancer
7q21.2	rs6964587, rs10644111, rs35417517	AKAP9, LRRD1, CYP51A1-AS1	rs1011372	AKAP9	Active promoter and active enhancer
7q21.2	rs35522438, rs35417517, rs10644111, rs6964587	AKAP9, LRRD1, CYP51A1-AS1, KRIT1	rs5885795	AKAP9	Active promoter and active enhancer
7q21.2	rs35522438, rs35417517, rs10644111, rs6964587	AKAP9, LRRD1, CYP51A1-AS1, KRIT1	rs4727266	AKAP9	Active promoter and active enhancer
7q21.2	rs35522438, rs35417517, rs10644111, rs6964587	AKAP9, LRRD1, CYP51A1-AS1, KRIT1	rs4727267	AKAP9	Active promoter and active enhancer
7q21.2	rs35522438, rs35417517, rs10644111, rs6964587	AKAP9, LRRD1, CYP51A1-AS1, KRIT1	rs6465339	AKAP9	Active promoter and active enhancer
7q21.2	rs35522438, rs35417517, rs10644111, rs6964587	AKAP9, LRRD1, CYP51A1-AS1, KRIT1	rs4279	AKAP9	Active promoter and active enhancer
7q21.2	rs35522438, rs35417517, rs10644111, rs6964587	AKAP9, LRRD1, CYP51A1-AS1, KRIT1	rs12704637	AKAP9	Active promoter and active enhancer
11p15.5	rs6597981	PIDD1	rs7942564	GATD1	Active promoter and active enhancer
11p15.5	rs6597981	PIDD1	rs7948070	GATD1	Active promoter and active enhancer
11q13.1	rs3903072	SNX32, OVOL1	rs4621	CFL1, SNX32#	Active promoter and active enhancer
11q13.1	rs3903072	SNX32, OVOL1	rs7125986	CFL1, SNX32#	Active promoter
11q13.1	rs3903072	SNX32, OVOL1	rs7947929	CFL1, SNX32#	Active promoter
11q13.1	rs3903072	SNX32, OVOL1	rs7947741	CFL1, SNX32#	Active promoter
11q13.1	rs3903072	SNX32, OVOL1	rs13817	CFL1, SNX32#	Active promoter and active enhancer
19p13.11	rs8170	BABAM1	rs3745187	ABHD8	Active promoter
19p13.11	rs2965183, rs2304098	GATAD2A, YJEFN3	rs3934667	MAU2	Active promoter
Continued					

Chr_band	GWAS variant	GWAS nearest gene	Candidate causal variants	daeQTL gene	Regulatory feature
19p13.11	rs2965183, rs2304098	GATAD2A, YJEFN3	rs2916068	MAU2	Active promoter
19p13.11	rs2965183, rs2304098	GATAD2A, YJEFN3	rs80007081	YJEFN3#, CILP2#, ENSG00000258674#	Active promoter and active enhancer
19p13.11	rs2965183, rs2304098	GATAD2A, YJEFN3	rs17684164	YJEFN3#, CILP2#, ENSG00000258674#	Active promoter and active enhancer
19p13.11	rs2965183, rs2304098	GATAD2A, YJEFN3	rs77254326	YJEFN3#, CILP2#, ENSG00000258674#	Active promoter and active enhancer
C. Loci for which no target gene could be pointed					
6p22.1	rs9257408	KRT18P1	rs209174	NA	Active promoter and active enhancer
6p22.1	rs9257408	KRT18P1	rs209173	NA	Active promoter and active enhancer
6p22.1	rs9257408	KRT18P1	rs3135315	NA	Active promoter and active enhancer
6p22.1	rs9257408	KRT18P1	rs184093	NA	Active promoter and active enhancer
6p22.1	rs9257408	KRT18P1	rs209138	NA	Active promoter
6p22.1	rs9257408	KRT18P1	rs3131102	NA	Active promoter
17q23.1	rs61495451	VMP1	rs3803863	chr17:59,852,174	Active promoter
17q23.1	rs61495451	VMP1	rs2333562	chr17:59,852,174	Active promoter and active enhancer
17q23.1	rs61495451	VMP1	rs138148328	chr17:59,852,174	Active enhancer
19p13.11	rs4808801, rs172032, rs7258465	ELL, SSBP4	rs28375303	chr19:18,416,447	Active promoter
19p13.11	rs4808801, rs172032, rs7258465	ELL, SSBP4	rs271621	chr19:18,416,447	Active promoter and active enhancer

Table 2. Loci with candidate risk rSNPs and novel suggested target genes. *Reported as rs116095464 in the original GWAS. #Linkage disequilibrium (LD) values r^2 between the daeQTL and the GWAS risk variant in the European population. §Gene not expressed in breast mammary tissue or without expression information in GTEx. #Novel suggested target gene in loci with previously suggested target genes. §Gene not expressed in breast mammary tissue or without expression information in GTEx.

rs226198 impacts the binding of both factors and H3K4me3 deposition or whether this epigenetic mark is a consequence of altered transcription, as previously suggested[55,56]. The minor T-allele of rs6880209 also showed preferential binding by MYC (4.8-fold, $p < 2.2e{-}16$) and MAX (2.4-fold, $p = 2.7e{-}03$), with smaller fold-change differences than rs226198, and additional preferential binding by POL2 (2.6-fold, $p = 1.27e{-}06$) in MCF7 cells. However, similar to rs111549985, DHS preferentially occurred in the major/reference C-allele in T47D cells (5.3-fold, $p = 9.1e{-}04$) (Fig. 6c, Table S12). Interestingly, the expression of *MAX* correlated with *ATG10, RPS23* and *ATP6AP1L,* and the expression of *MYC* correlated with the expression of *ATG10* (Fig. S16). Furthermore, the expression levels of *ATG10* and *ATP6AP1L* were positively correlated in breast tissue from healthy women (top 2.5% quantile of 500,000 pairwise tests) and in normal-matched tissue from patients with BC (Fig. S17). The observation that *ATG10* and *ATP6AP1L* are in different topologically associating domains (TADs) and that the candidate causal variants rs226198 and rs6880209 fall on the boundary between them (Fig. S18) suggests that a shared pattern of chromatin condensation does not drive the correlated gene expression but instead by a shared cis-regulatory sequence.

Since genetic variants affecting mRNA decay or alternative splicing[57] can cause allelic expression imbalances, we aimed to explore further the alternative transcription's role in gene expression regulation and driving risk at the 5q14.1 locus. To accomplish this, we performed an sQTL analysis for *ATG10* that was not restricted to the candidate risk rSNPs but included all SNPs located within 5 kb upstream and downstream of *ATG10* to increase the stringency of the exercise.

We identified six sQTLs (FDR ≤ 5%) in the tumour data, whose minor alleles were associated with changes in the expression of two protein-coding isoforms: decreased expression of ENST00000458350 (one extra exon) and increased expression of ENS3′UTR0282185 (longer 3′ UTR) (Fig. 7, Fig. S19a, Table S13). Interestingly, ENST00000282185 is expressed at significantly lower levels in tumours than in normal-matched tissue, in line with the reported oncogenic effect of UTR length[58], although with a small effect size (fold-change = 1.20) (Fig. S20). The strong correlation between sQTL q-values and LD with the lead GWAS SNP rs7707921 (r = 0.94, p-value = 3.15E−12, Fig. S18b) supports the contribution of alternative transcription of *ATG10* to BC risk. Although no sQTL was detected for *ATG10* in normal breast data (Table S13), sQTL nominal p-values and LD with rs7707921 were still correlated in normal matched breast samples (r = 0.59, p-value = 0.002) (Fig. S21). *ATP6AP1L* did not display sufficient alternative transcription dispersion to allow the sQTL analysis. Subsequent functional analysis of ATG10's sQTLs, and their proxy SNPs (LD r2 ≥ 0.95), revealed the prediction of rs111549985 (5′ UTR) and rs6884232 (3′ UTR) to cause a riboSNitch (a functional RNA structure disrupted by an SNP[46]). Although RBP binding data for breast tissue do not exist, these variants have been reported to disrupt the binding of Xrn2 (involved in termination by RNA polymerase II) and of Igf2bp1 (a translation regulator) in K562 cells (Tables S14, S15), which would require confirmation in breast cells.

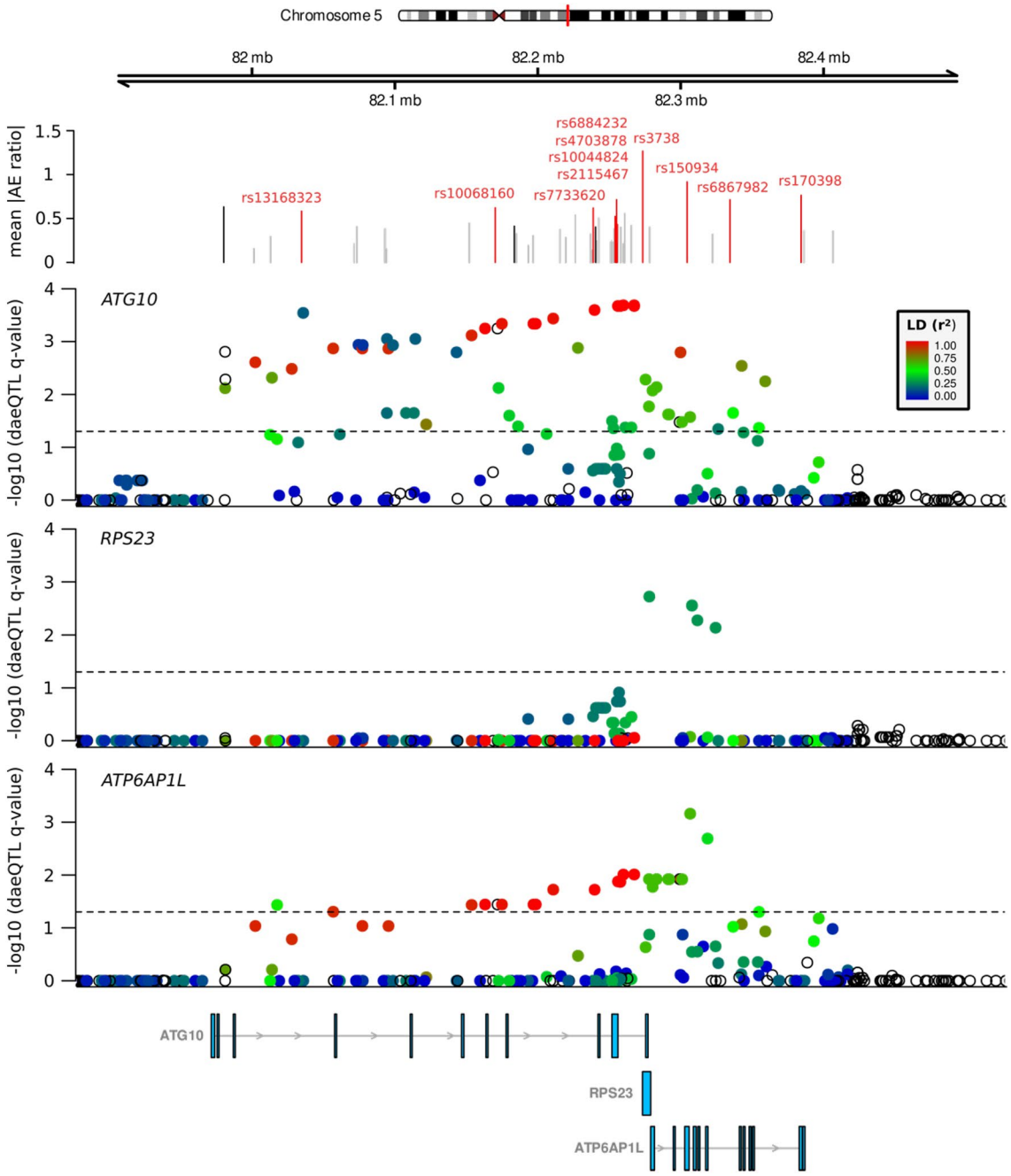

Fig. 5. Evidence of DAE and daeQTL analysis at the 5q14.1 BC risk locus. The top track shows the mean values of the absolute AE ratios measured at aeSNPs across the region, with the non-daeSNPs shown in grey, the daeSNPs in black and the daeSNPs with mapped daeQTLs in red. The subsequent tracks show the daeQTL mapping corrected p-values for *ATG10*, *RPS23* and *ATP6AP1L*.

Risk model for 5q14.1 links higher expression of *ATG10* and *ATP6AP1L* with protection against BC

Haplotype analysis of the samples included herein revealed two common haplotypes: one harbouring the major alleles of all proposed risk-rSNPs and the GWAS lead SNP rs7707921 (frequency of 71.1%) and another with the corresponding minor alleles (frequency of 21.9%) (Fig. S22). The proposed risk-rSNPs are among the most significant eQTLs for the two genes: rs111549985 for *ATG10* and rs6880209 for *ATP6AP1L* (Fig. S23)[59]. Therefore, the most common haplotype is associated with an increased risk for BC and lower expression of *ATG10* and *ATP6AP1L* (Fig. S22).

Our proposed model for risk at 5q14.1 (Fig. 8) establishes that the minor alleles of rs111549985, rs226198, and rs6880209 confer protection against BC by (1) increasing the binding of POL2 II to the promoter of *ATG10* (driven by rs111549985), (2) the binding of POL2 to the shared promoter of *RPS23/ATP6AP1L* (driven by rs6880209), and (3) the binding of cMYC and MAX to a regulatory region (possible enhancer) (driven by

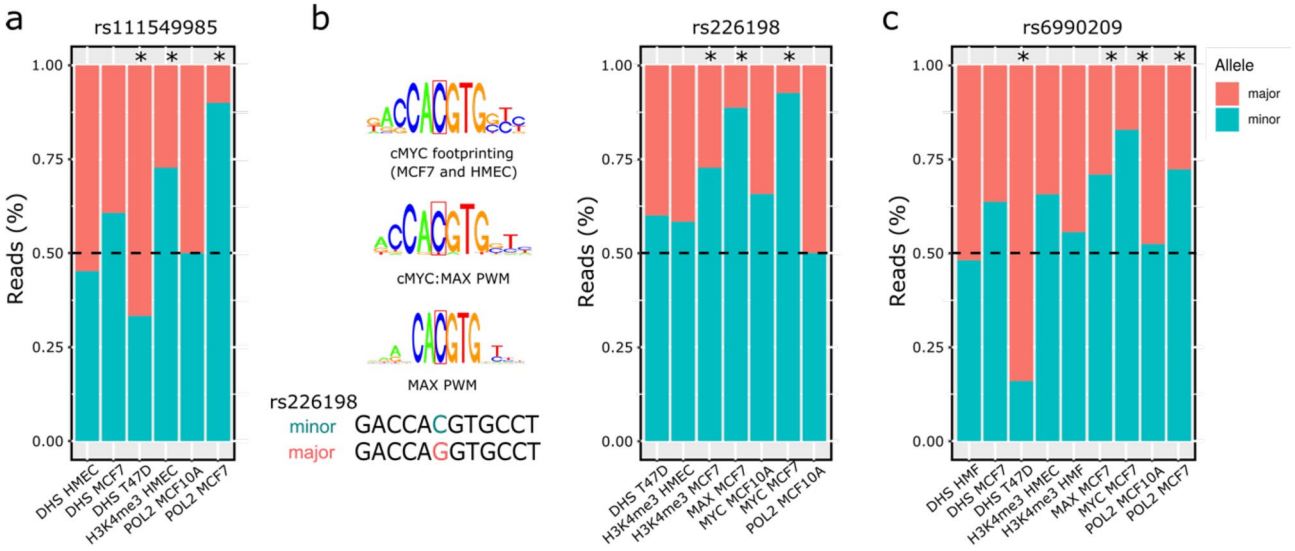

Fig. 6. Variants at the 5q14.1 risk locus associated with differential transcription factor binding. Allele-specific analysis of the effect of three candidate risk rSNPs—(**a**) rs111549985, (**b**) rs226198 and (**c**) rs6880209—on RNA polymerase II (POL2) and transcription factor (TF) binding, DNase I targeting (DHS) and H3K4me3 modification in different heterozygous cell lines. An asterisk indicates statistically significant imbalances (two-sided binomial test, p-value ≤ 0.05). *HMEC* human mammary epithelial cells, *MCF7* human breast (adenocarcinoma) cell line, *T47D* human breast tumour cell line, *MCF10A* human breast epithelial cell line.

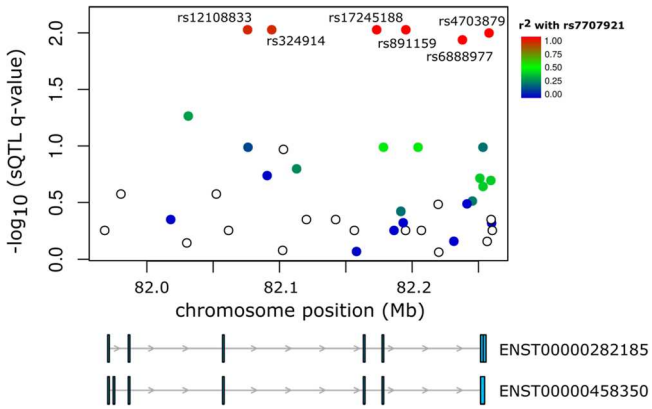

Fig. 7. Variants at the 5q14.1 risk locus associated with alternative transcription. Six sQTLs in high LD with rs7707921 were identified for *ATG10*. The −log10(q-value) for the sQTL analysis (y-axis) is shown for the 5q14.1–14.2 region (hg38). Colour intensity represents the LD (r^2) between the analysed variants and the GWAS lead SNP rs7707921. Below are two *ATG10* transcripts whose expression ratios are associated with the sQTLs.

rs226198), increasing the expression of *ATG10* and *ATP6AP1L*. These results reveal a complex regulatory landscape at the 5q14.1–14.2 locus, with multiple independent causal variants.

Discussion

Here, we present the first genome-wide map of differentially expressed allelic genes (daeGenes) and their genetic determinants (daeQTLs) in normal breast tissue. We found widespread differential allelic expression (DAE) across the genome and identified daeQTLs for 26% of daeGenes. By intersecting this map with GWAS data, we identified risk-daeQTLs and target genes for 93 BC risk loci. Next, we retrieved epigenetic regulatory annotations on all candidate risk-rSNPs (risk-daeQTLs and their proxies in high LD) to prioritise variants with regulatory potential for further functional analysis. We identified 406 variants with strong regulatory potential annotated to 55 different chromosomal bands and candidates for regulating the expression levels of 96 genes. Our results represent a practical and valuable resource for prioritising loci for follow-up GWASs. As a proof of concept, we functionally characterised the 5q14.1–14.2 BC risk locus in depth and proposed four causal regulatory variants targeting the genes *ATG10* and *ATP6AP1L* acting via multiple allele-specific mechanisms. Our results suggest a complex regulatory landscape underlying BC aetiology.

We show that cis-acting variants regulate the expression of 65% of genes in normal breast tissue, with some genes displaying extreme allelic differences of up to 32-fold. Notably, we identified a novel gene with monoallelic

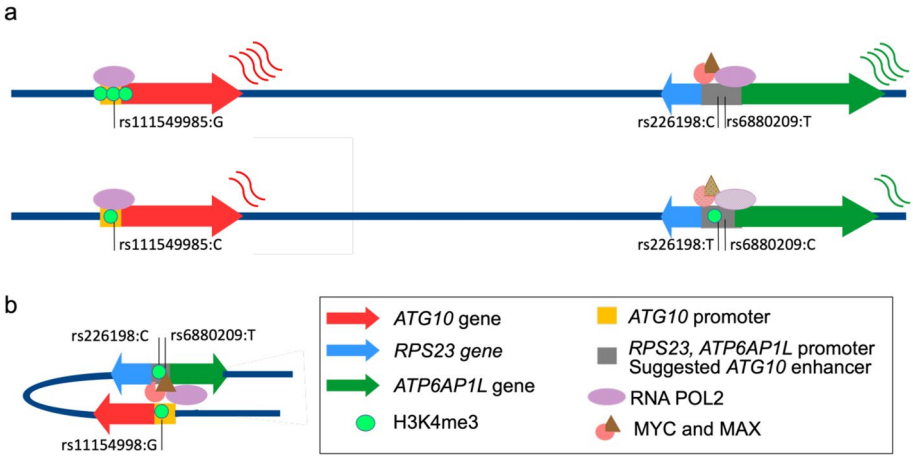

Fig. 8. Complex risk regulatory landscape of the 5q14.1 locus. (**a**) Levels of expression of *ATG10* and *ATP6AP1L* genes differ between the haplotypes containing either the minor alleles of rs111549985, rs226198 and rs6880209 (above) or the major ones (below). Coloured arrows indicate the direction of transcription of the individual genes, the saturation of the corresponding colours indicates the strength of protein binding, the number of green circles indicates the level of H3K4me3 and the coloured curvy lines indicate the relative levels of transcript produced. (**b**) Schematic representation of the proposed model for the positive correlation between *ATG10* and *ATP6AP1L* via a shared regulatory region.

expression, *ARCN1*, which warrants further inspection to confirm its imprinting status. An enrichment of daeSNPs at intergenic and intronic regions, as well as noncoding transcripts, noncoding genes, and pseudogenes, concurs with previous reports of predominant allelic imbalances of expression at gene-depleted regions and genes under fewer evolutionary constraints[60,61].

To overcome the lack of phasing information, we applied two different tests in the daeQTL mapping, according to the AE ratio distribution, which led to the identification of 54,357 variants associated with AE ratios for 6761 genes, both coding and noncoding for proteins. The stringent statistical correction and the use of distance as a covariate in the second mapping approach increased its confidence level but limited the statistical power to identify regulatory variants in lower LD with the daeSNP or located more distally.

We found evidence of expression regulation by cis-acting variants for most reported GWAS loci and believe that alternative mechanisms are at play in the remainder. We identified risk-daeQTLs at 93 different loci, including 72 loci with novel candidate risk target genes (including *NEK10* at 3p24.1 and *ZBED6* and *ZC3H11A* at 1q32.1). Moreover, the initial daeQTL map in normal breast tissue can be further mined whenever new risk variants are identified through GWAS. These results offer a resource platform for functional studies of causal variants and target genes and can help uncover the role of cis-regulatory variation in BC risk.

Finally, we conducted an in silico functional analysis of the 5q14.1–14.2 BC risk locus and identified three strong candidate causal variants: rs111549985, rs226198, and rs6880209. We predict that these variants functionally impact TF binding, chromatin state, and gene expression levels of *ATG10* and *ATP6AP1L*. A similar involvement of diverse regulatory mechanisms has been suggested previously for other BC risk loci[4,62,63]. Both A*TG10* (involved in autophagy) and the *ATP6AP1L* pseudogene have been suggested to have roles in cancer[64–67]. A variant at *ATG10* (rs7313473) was previously associated with BC risk by regulating promoter activity, and *ATG10* was suggested to act as a tumour suppressor gene in breast tissue[68]. For *ATP6AP1L*, another variant (rs10514231) was reported to lead to *ATP6AP1L* downregulation by decreasing the binding affinity of TCF7L2 in an intronic regulatory region[67]. Although we did not find supporting evidence for the same variants, our results show an indirect association between the lower expression of *ATG10* and *ATP6AP1L* and BC risk, suggesting that the downregulation of these two genes may contribute to tumorigenesis.

The advantages of our analysis compared to previous reports of AE in normal breast and tumour tissue[16,18,19,69] include using the most significant number of normal breast tissue samples, the genome-wide approach, and the mapping of candidate regulatory variants. We found a similar frequency of daeSNPs to previous reports in other tissues/cell lines but a higher frequency of daeGenes[13,17,18,70]. This higher frequency of daeGenes could be due to our ability to identify genes regulated by common cis-acting variants with weak to large effect sizes[19], a consequence of the imposed conditions to call DAE (allelic change difference of 1.5-fold and the minimum number of heterozygotes). Additionally, we did not integrate the AE ratios of multiple daeSNPs in the same gene due to the absence of phase data and to maximise the information withdrawn from daeSNPs that might be located in different LD blocks. The complex regulatory landscape we identified at the 5q14.1 locus, with multiple cis-acting variants located in the same haplotypes and AE likely resulting from the sum of the effects of each variant, supports this analysis approach. Furthermore, as we propose, a global measure of the AE imbalance at each gene would impair the mapping of daeQTLs at individual daeSNPs and restrict the analysis to genes with multiple daeSNPs. Finally, besides the more commonly studied protein-coding genes, we analysed noncoding genes and pseudogenes, such as *ATP6AP1L*.

Our results confirm the advantage of using DAE analysis to detect the effect of rSNPs compared to eQTL analysis, as shown by the higher number of daeGenes than eGenes among gwasGenes[71–73]. As a minority of gwasGenes were exclusively eGenes, we believe that DAE and eQTL analyses are complementary and should be used in parallel when possible.

Our use of microarray data could be seen as a limitation compared to RNA-seq data, which have more extensive transcriptome coverage and high quantification accuracy for more extreme allelic imbalances. However, microarrays are a widely used and precise technology for measuring AE[13,16,22], as we confirmed with our validated monoallelic expression of known imprinted genes and with independent PCR analysis. The only publicly available RNA-seq dataset with normal breast tissue is from the GTEx project. However, our approach presents several advantages: (1) we processed and hybridised the DNA and RNA samples in parallel to minimise technical issues, (2) we used total RNA, which includes coding/noncoding genes and spliced/unspliced transcripts, and (3) we showed that the range of gene expression levels of daeGenes was comparable to that of the eGenes from the GTEx dataset. The following steps will be to carry out matched RNA-seq and DNA-seq to combine all the advantages mentioned above and expand the discovery of daeGenes and rSNPs.

While our approach of defining risk-daeQTLs based on LD with GWAS index SNPs provides valuable insights and a potential link, it does not establish causality. Future work should address this limitation by performing co-localization analysis for all identified risk-daeQTL loci.

Our study predominantly analysed samples from individuals of European ancestry, and we combined these results with GWAS findings that included European populations for consistency. However, leveraging a multi-ancestry study design in future research is essential. Different ancestral populations possess distinct genetic backgrounds, unique sets of genetic variants and varying frequencies of shared variants. Incorporating data from multiple ancestries can broaden our understanding of the genetic and regulatory mechanisms underlying breast cancer risk[19,74].

Here, we provide a genome-wide list of variants with strong regulating potential for normal breast tissue, a valuable resource for researchers prioritising GWAS results for functional characterisation and those interested in other BC-related traits. The extensive characterisation of the regulatory landscape at the 5q14.1 BC risk locus identified candidate causal variants and revealed the multiple mechanisms involved. Further studies of this locus will elucidate the mechanisms involved and the relative contributions of each variant and target gene to the genetic risk. Overall, our results reinforce the importance of cis-regulatory variation as a major player in BC susceptibility and the power of identifying these variants in the disease's tissue of origin—normal breast tissue. They also show that multiple causal variants may co-occur and act via independent cis-regulatory mechanisms at BC risk loci, supporting a broader approach to functional studies.

Data availability

The datasets supporting the conclusions of this article are available in the following repositories: GWAS Catalog [https://www.ebi.ac.uk/gwas], Ensembl database (annotated to GRCh38.p13) [https://www.ensembl.org], GTEx Project (v7 and v8) [https://www.gtexportal.org], microarray data from GEO [https://www.ncbi.nlm.nih.gov/geo/] under accession number GSE35023.

Code availability

We used R to carry out the DAE and daeQTL mapping analyses, the code of which is available on GitHub (https://github.com/maialab/DaeBreastMicroarrays).

Received: 1 February 2024; Accepted: 4 September 2024
Published online: 28 September 2024

References

1. Wendt, C. & Margolin, S. Identifying breast cancer susceptibility genes—A review of the genetic background in familial breast cancer. *Acta Oncol.* **58**, 1–12 (2019).
2. Gallagher, M. D. & Chen-Plotkin, A. S. The post-GWAS era: From association to function. *Am. J. Hum. Genet.* **102**, 717–730 (2018).
3. Maurano, M. T. *et al.* Systematic localization of common disease-associated variation in regulatory DNA. *Science* **337**, 1190–1195 (2012).
4. Fachal, L. *et al.* Fine-mapping of 150 breast cancer risk regions identifies 191 likely target genes. *Nat. Genet.* **52**, 56–73 (2020).
5. Meyer, K. B. *et al.* Allele-specific up-regulation of FGFR2 increases susceptibility to breast cancer. *PLoS Biol.* **6**, e108 (2008).
6. Udler, M. S. *et al.* Fine scale mapping of the breast cancer 16q12 locus. *Hum. Mol. Genet.* **19**, 2507–2515 (2010).
7. Meyer, K. B. *et al.* A functional variant at a prostate cancer predisposition locus at 8q24 is associated with PVT1 expression. *PLoS Genet.* **7**, e1002165 (2011).
8. Darabi, H. *et al.* Polymorphisms in a putative enhancer at the 10q21.2 breast cancer risk locus regulate NRBF2 expression. *Am. J. Hum. Genet.* **97**, 22–34 (2015).
9. Michailidou, K. *et al.* Association analysis identifies 65 new breast cancer risk loci. *Nature* **551**, 92–94 (2017).
10. Ghoussaini, M. *et al.* Evidence that the 5p12 variant rs10941679 confers susceptibility to estrogen-receptor-positive breast cancer through FGF10 and MRPS30 regulation. *Am. J. Hum. Genet.* **99**, 903–911 (2016).
11. Dunning, A. M. *et al.* Breast cancer risk variants at 6q25 display different phenotype associations and regulate ESR1, RMND1 and CCDC170. *Nat. Genet.* **48**, 374–386 (2016).
12. Pastinen, T., Ge, B. & Hudson, T. J. Influence of human genome polymorphism on gene expression. *Hum. Mol. Genet.* **15**, R9–R16 (2006).
13. Ge, B. *et al.* Global patterns of cis variation in human cells revealed by high-density allelic expression analysis. *Nat. Genet.* **41**, 1216–1222 (2009).
14. Forton, J. T. *et al.* Localization of a long-range cis-regulatory element of IL13 by allelic transcript ratio mapping. *Genome Res.* **17**, 82–87 (2007).
15. Bjornsson, H. T. *et al.* SNP-specific array-based allele-specific expression analysis. *Genome Res.* **18**, 771–779 (2008).

16. Gao, C. *et al.* Identifying breast cancer risk loci by global differential allele-specific expression (DASE) analysis in mammary epithelial transcriptome. *BMC Genom.* **13**, 570 (2012).
17. Romanel, A., Lago, S., Prandi, D., Sboner, A. & Demichelis, F. ASEQ: Fast allele-specific studies from next-generation sequencing data. *BMC Med. Genom.* **8**, 9 (2015).
18. Przytycki, P. F. & Singh, M. Differential allele-specific expression uncovers breast cancer genes dysregulated by cis noncoding mutations. *Cell Syst.* **10**, 193–203 (2020).
19. Aguet, F. *et al.* Genetic effects on gene expression across human tissues. *Nature* **550**, 204–213 (2017).
20. Hamdi, Y. *et al.* Association of breast cancer risk with genetic variants showing differential allelic expression: Identification of a novel breast cancer susceptibility locus at 4q21. *Oncotarget* **5**, 80140–80163 (2014).
21. Zhang, Y. *et al.* Integrative genomic analysis predicts causative cis-regulatory mechanisms of the breast cancer-associated genetic variant rs4415084. *Cancer Res.* **78**, 1579–1591 (2018).
22. Liu, R. *et al.* Allele-specific expression analysis methods for high-density SNP microarray data. *Bioinformatics* **28**, 1102–1108 (2012).
23. Du, P. *et al.* Comparison of Beta-value and M-value methods for quantifying methylation levels by microarray analysis. *BMC Bioinform.* **11**, 587 (2010).
24. Gimelbrant, A., Hutchinson, J. N., Thompson, B. R. & Chess, A. Widespread monoallelic expression on human autosomes. *Science* **318**, 1136–1140 (2007).
25. Maia, A.-T. *et al.* Extent of differential allelic expression of candidate breast cancer genes is similar in blood and breast. *Breast Cancer Res.* **11**, R88 (2009).
26. Li, Y., Willer, C. J., Ding, J., Scheet, P. & Abecasis, G. R. MaCH: Using sequence and genotype data to estimate haplotypes and unobserved genotypes. *Genet. Epidemiol.* **34**, 816–834 (2010).
27. Xiao, R. & Scott, L. J. Detection of cis-acting regulatory SNPs using allelic expression data. *Genet. Epidemiol.* **35**, 515–525 (2011).
28. Hochberg, Y. & Benjamini, Y. More powerful procedures for multiple significance testing. *Stat. Med.* **9**, 811–818 (1990).
29. Ignatiadis, N., Klaus, B., Zaugg, J. & Huber, W. Data-driven hypothesis weighting increases detection power in genome-scale multiple testing. *Nat. Methods* **13**, 577–580 (2016).
30. MacArthur, J. *et al.* The new NHGRI-EBI catalog of published genome-wide association studies (GWAS Catalog). *Nucleic Acids Res.* **45**, D896–D901 (2017).
31. Magno, R. & Maia, A.-T. gwasrapidd: An R package to query, download and wrangle GWAS catalog data. *Bioinformatics* **36**, 649 (2019).
32. Yates, A. *et al.* The ensembl REST API: Ensembl data for any language. *Bioinformatics* **31**, 143–145 (2015).
33. Goovaerts, T. *et al.* A comprehensive overview of genomic imprinting in breast and its deregulation in cancer. *Nat. Commun.* **9**, 4120 (2018).
34. Consortium TGte *et al.* The genotype-tissue expression (GTEx) pilot analysis: Multitissue gene regulation in humans. *Science* **348**, 648–60 (2015).
35. Dunham, I. *et al.* An integrated encyclopedia of DNA elements in the human genome. *Nature* **489**, 57–74 (2012).
36. Kundaje, A. *et al.* Integrative analysis of 111 reference human epigenomes. *Nature* **518**, 317–330 (2015).
37. Kent, W. J. *et al.* The human genome browser at UCSC. *Genome Res.* **12**, 996–1006 (2002).
38. Gonzalez, J. N. *et al.* The UCSC genome browser database: 2021 update. *Nucleic Acids Res.* **49**, D1046–D1057 (2021).
39. Ward, L. D. & Kellis, M. HaploReg: A resource for exploring chromatin states, conservation, and regulatory motif alterations within sets of genetically linked variants. *Nucleic Acids Res.* **40**, D930–D934 (2012).
40. Boyle, A. P. *et al.* Annotation of functional variation in personal genomes using RegulomeDB. *Genome Res.* **22**, 1790–1797 (2012).
41. Thorvaldsdóttir, H., Robinson, J. T. & Mesirov, J. P. Integrative genomics viewer (IGV): High-performance genomics data visualization and exploration. *Brief. Bioinform.* **14**, 178–192 (2013).
42. Storey, J., Bass, A., Dabney, A. & Robinson, D. *qvalue: Q-Value Estimation for False Discovery Rate Control*. http://github.com/jdstorey/qvalue (2021).
43. Monlong, J., Calvo, M., Ferreira, P. G. & Guigó, R. Identification of genetic variants associated with alternative splicing using sQTLseekeR. *Nat. Commun.* **5**, 4698 (2014).
44. Zhu, Y. *et al.* POSTAR2: Deciphering the post-transcriptional regulatory logics. *Nucleic Acids Res.* **47**, D203–D211 (2019).
45. Mao, F. *et al.* RBP-Var: A database of functional variants involved in regulation mediated by RNA-binding proteins. *Nucleic Acids Res.* **44**, D154–D163 (2016).
46. Corley, M., Solem, A., Qu, K., Chang, H. Y. & Laederach, A. Detecting riboSNitches with RNA folding algorithms: A genome-wide benchmark. *Nucleic Acids Res.* **43**, 1859–1868 (2015).
47. Paz, I., Kosti, I., Ares, M., Cline, M. & Mandel-Gutfreund, Y. RBPmap: A web server for mapping binding sites of RNA-binding proteins. *Nucleic Acids Res.* **42**, W361–W367 (2014).
48. Barrett, J. C., Fry, B., Maller, J. & Daly, M. J. Haploview: Analysis and visualization of LD and haplotype maps. *Bioinformatics* **21**, 263–265 (2005).
49. Colaprico, A. *et al.* TCGAbiolinks: An R/Bioconductor package for integrative analysis of TCGA data. *Nucleic Acids Res.* **44**, e71 (2016).
50. Seitz, H. *et al.* Imprinted microRNA genes transcribed antisense to a reciprocally imprinted retrotransposon-like gene. *Nat. Genet.* **34**, 261–262 (2003).
51. Tierling, S. *et al.* High-resolution map and imprinting analysis of the Gtl2–Dnchc1 domain on mouse chromosome 12. *Genomics* **87**, 225–235 (2006).
52. Hagan, J. P., O'Neill, B. L., Stewart, C. L., Kozlov, S. V. & Croce, C. M. At least ten genes define the imprinted Dlk1-Dio3 cluster on mouse chromosome 12qF1. *PLoS ONE* **4**, e4352 (2009).
53. Michailidou, K. *et al.* Genome-wide association analysis of more than 120,000 individuals identifies 15 new susceptibility loci for breast cancer. *Nat. Genet.* **47**, 373–380 (2015).
54. Dang, C. V. MYC on the path to cancer. *Cell* **149**, 22–35 (2012).
55. Floc'hlay, S. *et al.* Cis-acting variation is common across regulatory layers but is often buffered during embryonic development. *Genome Res.* **31**, 120 (2020).
56. Howe, F. S., Fischl, H., Murray, S. C. & Mellor, J. Is H3K4me3 instructive for transcription activation? *Bioessays* **39**, 1–12 (2017).
57. Robles-Espinoza, C. D., Mohammadi, P., Bonilla, X. & Gutierrez-Arcelus, M. Allele-specific expression: Applications in cancer and technical considerations. *Curr. Opin. Genet. Dev.* **66**, 10–19 (2021).
58. Mayr, C. & Bartel, D. P. Widespread shortening of 3′ UTRs by alternative cleavage and polyadenylation activates oncogenes in cancer cells. *Cell* **138**, 673–684 (2009).
59. Lonsdale, J. *et al.* The genotype-tissue expression (GTEx) project. *Nat. Genet.* **45**, 580–585 (2013).
60. Campbell, C. D., Kirby, A., Nemesh, J., Daly, M. J. & Hirschhorn, J. N. A survey of allelic imbalance in F1 mice. *Genome Res.* **18**, 555–563 (2008).
61. Tung, J., Fédrigo, O., Haygood, R., Mukherjee, S. & Wray, G. A. Genomic features that predict allelic imbalance in humans suggest patterns of constraint on gene expression variation. *Mol. Biol. Evol.* **26**, 2047–2059 (2009).
62. Cox, D. G. *et al.* Common variants of the BRCA1 wild-type allele modify the risk of breast cancer in BRCA1 mutation carriers. *Hum. Mol. Genet.* **20**, 4732–4747 (2011).

63. Maia, A.-T. *et al.* Effects of BRCA2 cis-regulation in normal breast and cancer risk amongst BRCA2 mutation carriers. *Breast Cancer Res.* **14**, R63 (2012).
64. Jo, Y. K. *et al.* Increased expression of ATG10 in colorectal cancer is associated with lymphovascular invasion and lymph node metastasis. *PLoS ONE* **7**, e52705 (2012).
65. Wang, Y., Huang, J.-W., Castella, M., Huntsman, D. G. & Taniguchi, T. p53 is positively regulated by miR-542-3p. *Cancer Res.* **74**, 3218–3227 (2014).
66. Jo, Y. K. *et al.* Polypyrimidine tract-binding protein 1-mediated down-regulation of ATG10 facilitates metastasis of colorectal cancer cells. *Cancer Lett.* **385**, 21–27 (2017).
67. Ma, S., Ren, N. & Huang, Q. rs10514231 leads to breast cancer predisposition by altering ATP6AP1L gene expression. *Cancers* **13**, 3752 (2021).
68. Guo, X. *et al.* A comprehensive cis-eQTL analysis revealed target genes in breast cancer susceptibility loci identified in genome-wide association studies. *Am. J. Hum. Genet.* **102**, 890–903 (2018).
69. Zhang, K. *et al.* Digital RNA allelotyping reveals tissue-specific and allele-specific gene expression in human. *Nat. Methods* **6**, 613–618 (2009).
70. Ma, X. *et al.* Pan-cancer genome and transcriptome analyses of 1,699 paediatric leukaemias and solid tumours. *Nature* **555**, 371–376 (2018).
71. Adoue, V. *et al.* Allelic expression mapping across cellular lineages to establish impact of non-coding SNPs. *Mol. Syst. Biol.* **10**, 754 (2014).
72. Almlöf, J. C. *et al.* Powerful identification of cis-regulatory SNPs in human primary monocytes using allele-specific gene expression. *PLos ONE* **7**, e52260 (2012).
73. Pastinen, T. & Hudson, T. J. Cis-acting regulatory variation in the human genome. *Science* **306**, 647–650 (2004).
74. Martin, A. R. *et al.* Human demographic history impacts genetic risk prediction across diverse populations. *Am. J. Hum. Genet.* **100**, 635–649 (2017).

Acknowledgements

The authors would also like to thank Dr Nuno Barbosa-Morais at IMM for the excellent scientific discussions and the support given by the Unidade de Apoio à Investigação (UAIC) at Universidade do Algarve (UAlg), particularly Mr. Vitor Morais, and the Informatics Services of UAlg.

Author contributions

BAJP and ATM conceived the work, and RR, BAJP and ATM designed the work. BPA, CLR, NR, MOR, and ATM carried out laboratory experiments and acquired data. JMX, RM, BPA, AJF, RR, SS, MD, AMM and ATM analysed and interpreted data. JMX and ATM wrote the main manuscript text, and all authors reviewed the manuscript.

Funding

This work was supported by national Portuguese funding through FCT—Fundação para a Ciência e a Tecnologia and CRESC ALGARVE 2020, institutional support CBMR-UID/BIM/04773/2013, RISE—LA/P/0053/2020, UIDB/4255/2020—CINTESIS, POCI "01-0145-" EDER-022184 "GenomePT", the contract DL 57/2016/CP1361/CT0042 (J.M.X.) and individual postdoctoral fellowship SFRH/BPD/99502/2014 (J.M.X.). The research leading to these results has received funding from the People Programme (Marie Curie Actions) of the European Union's Seventh Framework Programme FP7/2007-2013/under REA Grant Agreement No. 303745 (A.T.M.), a Maratona da Saúde Award (A.T.M.) and a BCRF project Grant.

Competing interests

The authors declare no competing interests.

Additional information

Supplementary Information The online version contains supplementary material available at https://doi.org/10.1038/s41598-024-72163-y.

Correspondence and requests for materials should be addressed to J.M.X. or A.-T.M.

Reprints and permissions information is available at www.nature.com/reprints.

Publisher's note Springer Nature remains neutral with regard to jurisdictional claims in published maps and institutional affiliations.

Open Access This article is licensed under a Creative Commons Attribution-NonCommercial-NoDerivatives 4.0 International License, which permits any non-commercial use, sharing, distribution and reproduction in any medium or format, as long as you give appropriate credit to the original author(s) and the source, provide a link to the Creative Commons licence, and indicate if you modified the licensed material. You do not have permission under this licence to share adapted material derived from this article or parts of it. The images or other third party material in this article are included in the article's Creative Commons licence, unless indicated otherwise in a credit line to the material. If material is not included in the article's Creative Commons licence and your intended use is not permitted by statutory regulation or exceeds the permitted use, you will need to obtain permission directly from the copyright holder. To view a copy of this licence, visit http://creativecommons.org/licenses/by-nc-nd/4.0/.

© The Author(s) 2024